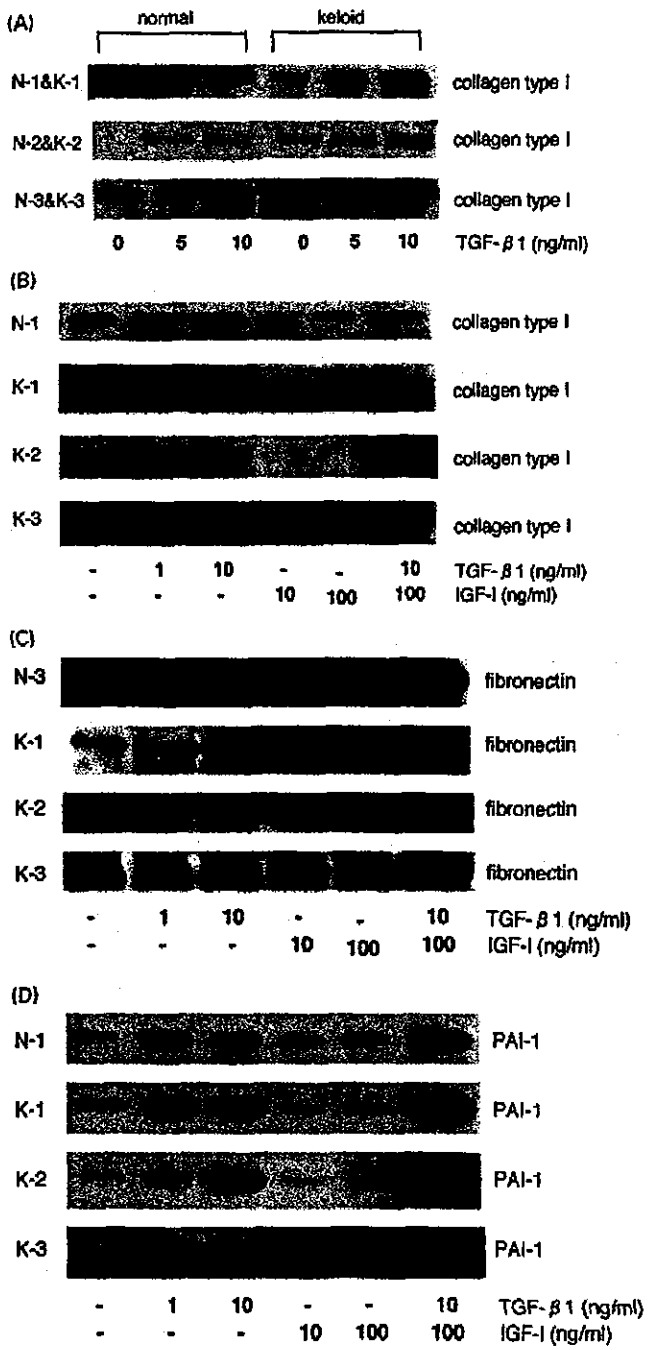

Figure 1. Western blotting of ECM proteins in culture media from dermal fibroblasts. (*A*) Concentration-dependent effect of TGF-β1 stimulation on collagen type I secretion by cultured human fibroblasts. *Lanes 1–3*: normal fibroblasts (N-1–3); *lanes 4–6*: keloid fibroblasts (K-1–3). Equivalent protein load was controlled by Bio-Rad protein assay kit. (*B*) Collagen type I expression after treatment with TGF-β1 (1 or 10 ng per ml) and IGF-I (10 or 100 ng per ml) separately, or in combination in normal (N-1) and keloid fibroblasts (K-1, 2). (*C*) Fibronectin expression after treatment with TGF-β1 (1 or 10 ng per ml), IGF-I (10 or 100 ng per ml), or both in combination in normal (N-3) and keloid fibroblasts (K-2, 3). (*D*) PAI-1 expression after treatment with TGF-β1 (1 or 10 ng per ml), IGF-I (10 or 100 ng per ml), or both in combination in normal (N-1) and keloid fibroblasts (K-1, 3).

reverse transcription–PCR. The combination treatment with TGF-β1 and IGF-I upregulated the expression of collagen type I mRNA in keloid fibroblasts nearly 2.2-fold compared with 1.5-fold in cells treated with TGF-β alone. In normal fibroblasts, this

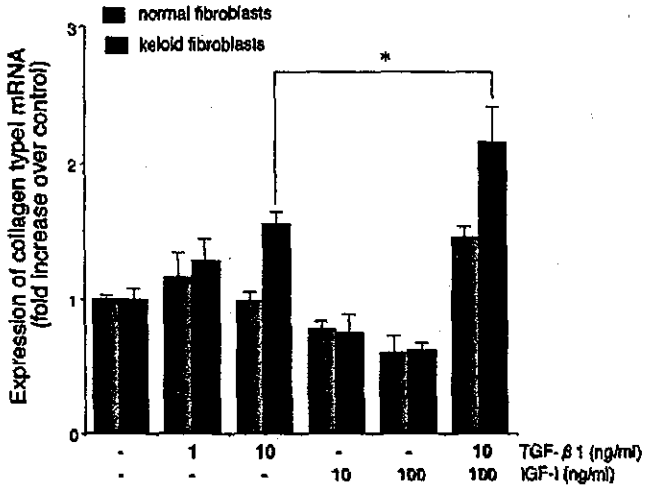

Figure 2. Expression of collagen type I mRNA after treatment with TGF-β1 (1 or 10 ng per ml), IGF-I (10 or 100 ng per ml) separately, or in combination in cultured fibroblasts. RNA was extracted from cultures, reverse transcribed, and analyzed by quantitative reverse transcription–PCR using real-time PCR. Results are expressed as fold increases of collagen I mRNA after normalization to α-tubulin. $^{*}p < 0.05$.

synergistic effect was not significant. IGF-I treatment alone, however, slightly downregulated the expression of collagen type I mRNA in both normal and keloid fibroblasts.

TGF-β signaling in mouse fibroblasts We treated BALB/C 3T3 mouse fibroblasts with TGF-β1 or IGF-I alone or in combination to assess whether Smad or p38 MAPK were acting dominantly downstream of the TGF-β1 receptor. **Figure 3**(*A*) shows that 10 ng IGF-I per ml treatment did not increase 3TP-Lux activity, whereas 100 ng IGF-I per ml treatment resulted in a small increase. TGF-β1 treatment (1 ng per ml or 10 ng per ml) produced an approximately 10-fold increase in activation. At the same time, the combination of the two factors increased 3TP-Lux activity approximately 25 times. 3TP-Lux activity was not increased by the combination treatment compared with TGF-β alone in HepG2 cells, indicating that the synergistic effect of TGF-β1 and IGF-I is cell-type specific.

We then determined whether the Smad cascades of TGF-β1 signaling were activated by IGF-I alone, or TGF-β1 and IGF-I in combination (**Fig 3***B*). TGF-β1 treatment (10 ng per ml) alone increased ARE activity in the presence of FAST-1, but TGF-β1 and IGF-I in combination did not further enhance the activity of ARE-Lux. ARE-Lux activity without FAST-1 cotransfection was unchanged by various combination treatments. In HepG2 cells, ARE-Lux activity was markedly induced by TGF-β1 treatment with FAST-1 cotransfection, but no synergistic effect was produced by TGF-β1/IGF-I combination.

3TP-Lux activity in human fibroblasts To confirm synergistic signal transduction in normal and keloid fibroblasts, we used the 3TP-Lux assay in normal and keloid fibroblasts. As shown in **Fig 4**, treatment with 100 ng per ml IGF-I did not enhance 3TP-Lux activity significantly, whereas 10 ng per ml TGF-β1 produced an increased activation of approximately 3- or 4-fold in normal and keloid fibroblasts, respectively. Furthermore, combination treatment produced a rise in activity of approximately 4-fold in normal fibroblasts, and an 8-fold increase in keloid fibroblasts.

Downstream signaling of TGF-β-induced MAPK cascades in human fibroblasts To examine the effect of intervention at various stages of the MAPK cascade on TGF-β1 and IGF-I signaling in human fibroblasts, we used SB203580 (a p38-specific inhibitor) and PD98059 (a MEK specific inhibitor). As

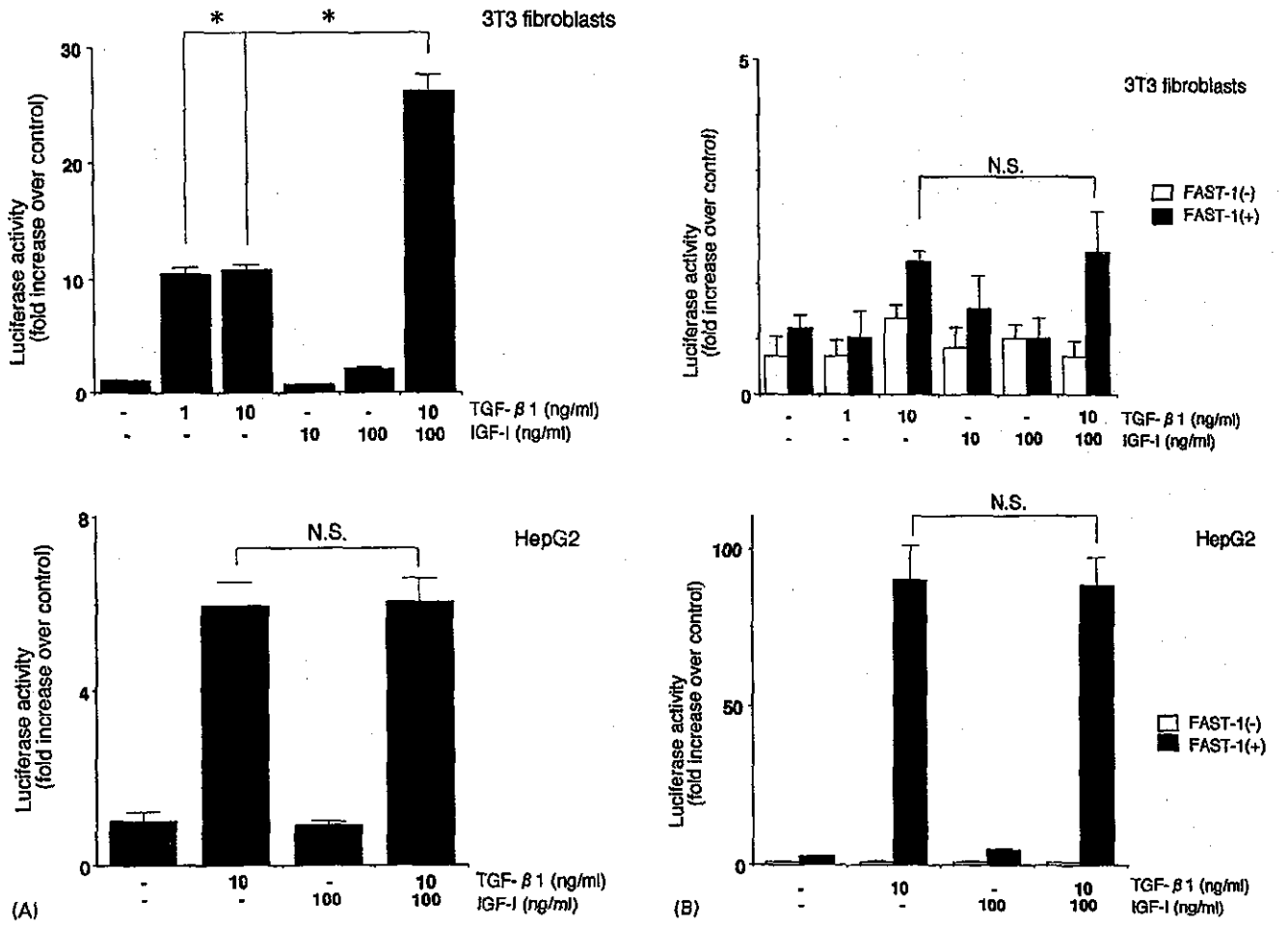

Figure 3. (*A*) **3TP-lux activity in BALB/C 3T3 mouse fibroblasts and HepG2 cells after treatment with TGF-β1 (1 or 10 ng per ml), IGF-I (10 or 100 ng per ml), or with both in combination.** *3T3 fibroblasts and HepG2 cells transfected with* 3TP-Lux were incubated for 12 h with various stimulants. (*B*) **ARE-lux activity in BALB/C 3T3 mouse fibroblasts and HepG2 cells after treatment with TGF-β1 (1 or 10 ng per ml), IGF-I (10 or 100 ng per ml) separately, or both in combination.** 3T3 fibroblasts and HepG2 cells were cotransfected with ARE-Lux in the presence or absence of FAST-1 before stimulation. *Results are expressed as fold increases above the values for untreated controls* (mean ± SE, n = 6). *p < 0.03, N.S., nonsignificant.

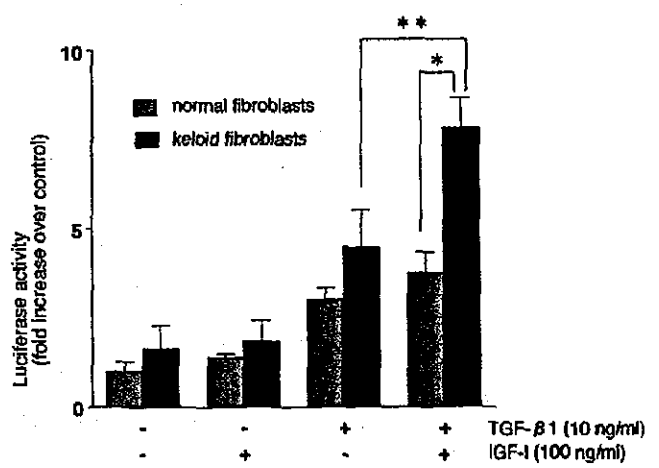

Figure 4. 3TP-lux activity in normal and keloid human fibroblasts treated with TGF-β1 (10 ng per ml), IGF-I (100 ng per ml) separately, or with both in combination. Normal and keloid fibroblasts transfected with 3TP-Lux were incubated 12 h with the stimulants. Results are expressed as fold increases above the values for untreated controls (mean ± SE, n = 6) in normal fibroblasts. *p < 0.01; **p < 0.03.

shown in **Fig 5**, the synergistic effect was almost completely blocked by SB203580, but not by PD98059, in both normal and keloid fibroblasts. Furthermore, *to examine whether* PI3K correlates with the enhancement of TGF-β signaling, we used wortmannin, a PI3K inhibitor. As shown in **Fig 6**, wortmannin almost abrogated the synergistic effect of IGF-I. We next examined whether phosphorylation of p38 and ATF-2 is enhanced by combination treatment with IGF-I and TGF-β1, as ATF-2 has been reported to be a common nuclear target of p38 MAPK pathways in TGF-β signaling (Gupta *et al*, 1995). TGF-β1 (10 ng per ml) doubled the level of phospho-ATF-2, and treatment with IGF-I and TGF-β1 enhanced it by approximately 3-fold (**Fig 7*A***). In contrast, treatment with IGF-I alone resulted in little change from control levels. Western blot analysis of phospho-p38 MAPK gave similar results: combination treatment markedly increased phosphorylation of p38 compared with either IGF-I or TGF-β1 treatment alone (**Fig 7*B***). Finally, we examined whether JNK activation correlates with synergistic effect of TGF-β and IGF-I; however, the phosphorylation level of JNK was not changed by various treatments (**Fig 7*C***).

DISCUSSION

In this study, the expression of collagen type I and fibronectin revealed that keloid fibroblasts are more responsive to synergistic

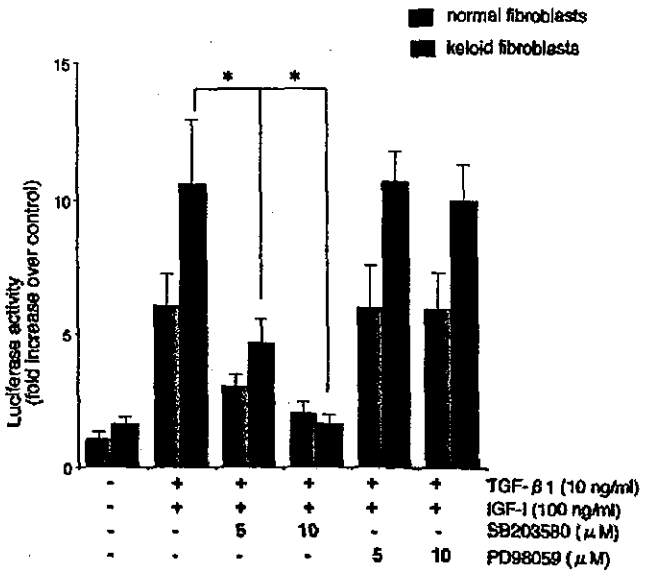

Figure 5. 3TP-lux activity in normal and keloid fibroblasts. The effect on MAPK pathways was examined by pretreatment with either PD98059 or SB203580 before administration of IGF-I (100 ng per ml), TGF-β1 (10 ng per ml) separately, or both in combination. PD98059 is a specific inhibitor of MEK1, and SB203580 is a specific inhibitor of p38. *$p < 0.03$

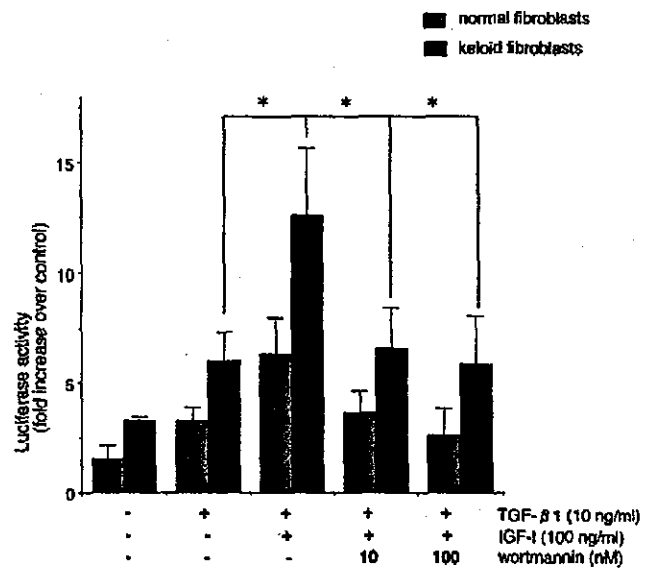

Figure 6. 3TP-lux activity in normal and keloid fibroblasts. The effect on PI3K pathways was examined by pretreatment with wortmannin (10 nM or 100 nM) before administration of IGF-I (100 ng per ml), TGF-β1 (10 ng per ml) or both in combination. Results are expressed as fold increases above the values for untreated controls (mean ± SE, $n = 6$). *$p < 0.03$.

stimulation induced by the combination of TGF-β1 and IGF-I than normal fibroblasts. Even on an mRNA level, real-time reverse transcription–PCR confirmed parallel collagen type I changes. Although the expression of collagen type I was slightly downregulated by IGF-I treatment alone on protein and mRNA levels, the combination of TGF-β and IGF-I enhanced its expression, suggesting that IGF-I plays a modulating role in TGF-β1-stimulated ECM protein secretion. Immunoblot analysis for PAI-1 demonstrated a synergistic effect of IGF-I with TGF-β1, suggesting that fibrosis may be accelerated as a result of suppression of fibrinolysis in keloids. To clarify the signaling mechanisms of this synergism, we employed the TGF-β *trans*-acting reporter system. 3TP-Lux activity was increased approximately 8-fold when keloid fibroblasts were treated with TGF-β1 and IGF-I, but not following treatment with IGF-I alone. Ghahary *et al* (2000) previously reported that IGF-I induces the expression of latent TGF-β1 through activation of c-*fos* and c-*jun* oncogenes; however, our data show that IGF-I stimulation alone did not increase the level of 3TP-Lux activity in time along with ECM protein production in keloid fibroblasts.

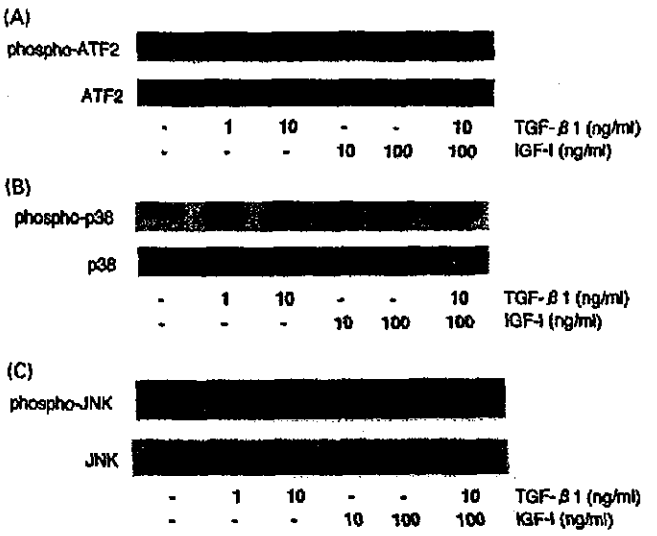

Figure 7. Western blotting showing phosphorylation of ATF-2, p38, and JNK after treatment with TGF-1 (1 or 10 ng per ml), IGF-I (10 or 100 ng per ml) separately, or both in combination in keloid fibroblasts.

Smad are a family of proteins that operate downstream of various members of the TGF-β superfamily (Heldin *et al*, 1997) with Smad2 and Smad3 being downstream effectors of the TGF-β signaling pathway. Upon ligand binding, they are phosphorylated by the TGF-β1 type I receptor kinase and translocate to the nucleus in a complex with Smad4 (Huang *et al*, 1995). This heteromeric complex may either bind directly to the promoters of its target genes, or associate with other transcription factors to induce gene transcription (Derynck *et al*, 1998). Recent work has identified a potential consensus Smad3-Smad4 DNA binding site, GTCTAGAC (Zawel *et al*, 1998), which is observed within the 3TP-Lux promoter and ARE-Lux promoter (Yingling *et al*, 1997; Dennler *et al*, 1998). This suggests that Smad pathways influence the activation of 3TP-Lux as do MAPK pathways. Recent studies revealed that Smad pathways are activated in the wound healing process, and may play some part in fibrosis (Verrecchia and Mauviel, 2002). To elucidate whether the synergistic effect of IGF-I on TGF-β1 signaling is mediated by Smad, we examined the ARE-Lux reporter system, both in the presence and absence of FAST-1. As FAST-1 specifically binds to Smad2, the FAST-1-dependent activation of the ARE-Lux promoter is mediated by endogenous Smad4 (Frey and Mulder, 1997). In this study, the ARE-Lux activity in the presence of FAST-1 increased approximately 80-fold over the control level in HepG2 cells, but only by approximately 2.5-fold in 3T3 fibroblasts, treated with TGF-β1. In addition, IGF-I did not enhance ARE-Lux activity in either HepG2 or 3T3 fibroblasts. Based on these results, it is plausible that MAPK predominantly influence ECM production by cultured fibroblasts treated with TGF-β and IGF-I, but Smad do not; however, Smad3 itself has been demonstrated to be involved in various fibrogenesis models, including keloids (Roberts *et al*, 2001; Chin *et al*, 2001). Further study is required to clarify the role of Smad3 in keloid formation.

Recently, we and other groups have reported that TGF-β1 can activate MAPK, ERK, and p38 protein kinase (Hanafusa *et al*,

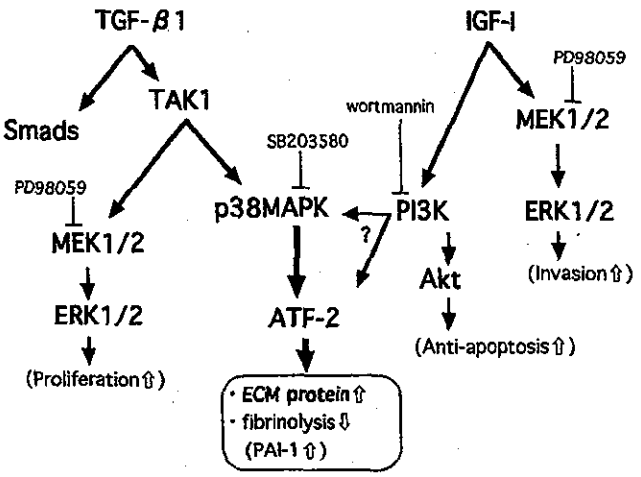

Figure 8. A possible molecular mechanism of keloid formation mediated by TGF-β1 and IGF-I cross-talk.

1999; Finlay *et al*, 2000; Ravanti *et al*, 2001; Akiyama-Uchida *et al* 2002; Sato *et al*, 2002). As TAK1 can activate the p38 MAPK pathway, we examined whether specific inhibitors of this signaling pathway can block 3TP-Lux activity. As shown in **Fig 5**, the synergistic effect of IGF-I and TGF-β1 was almost completely abrogated by the p38 inhibitor, SB203580, but not by the MEK inhibitor, PD98059, suggesting that p38 MAPK pathways are predominantly responsible for the regulation of induction of gene expression by TGF-β1. Alternatively, IGF-I activates MAPK pathways (ERK1/2) and PI3K pathways (Backer *et al*, 1992; Rozakis-Adcock *et al*, 1993; Skolnik *et al*, 1993). MEK inhibitor did not change the 3TP-Lux activity, indicating that the synergistic effect is independent on IGF-I/MEK/ERK pathway. As shown in **Fig 6**, the modulating effect of IGF-I was almost completely blocked by the PI3K specific inhibitor, wortmannin. Therefore, the specific inhibition of TGF-β1 signaling pathways suggests that PI3K pathways could be prevalent in the regulation of ECM production downstream of the IGF-I receptor. ATF-2, a member of the ATF/cyclic adenosine monophosphate response element binding protein (CREB) family of transcription factors, can form dimers through its leucine zipper structure and bind to CRE (Kara *et al*, 1990). p38 phosphorylates ATF-2 at Thr-69, Thr-71, and Ser-90 (Gupta *et al*, 1995). Our western blotting analysis demonstrated that phospho-ATF-2 was markedly increased by treatment with IGF-I and TGF-β1.

Although the precise cause of overexpression of IGF-IR in keloid fibroblasts is as yet unknown, it is highly possible that IGF-I/IGF-IR signaling could lead to characteristic keloid activities, such as proliferation, invasion, anti-apoptosis, and excess ECM production. **Figure 8** shows a proposed molecular mechanism of keloid formation mediated by TGF-β and IGF-I cross-talk. TGF-β stimulates cell proliferation via the ERK pathway (Pena *et al*, 2000). In previous studies, IGF-I has been associated with anti-apoptosis and invasive potential of keloid fibroblasts (Yoshimoto *et al*, 1999; Ishihara *et al* 2000). In this study, we have described a novel mechanism for keloid formation, in particular for the excess ECM production. IGF-I enhances fibrosis during keloid formation through TGF-β1 postreceptor signaling, predominantly via the p38 MAPK/ATF-2 pathway. The exact nature of this complex interaction between TGF-β and IGF-I involving cross-talk comprises a focus for further study on keloid formation.

This work was supported in part by a grant to Dr Yamashita from the Japanese Ministry of Education, Science and Culture (no. 12877286). We thank Dr Jeffrey L. Wrana for the kind donation of 3TP-Lux, ARE-Lux, and hFAST-1.

REFERENCES

Akiyama-Uchida Y, Ashizawa N, Ohtsuru A, *et al*: Norepinephrine enhances fibrosis mediated by TGF-β in cardiac fibroblasts. *Hypertension* 40:148–154, 2002

Babu M, Diegelmann RF, Oliver N: Keloid fibroblasts exhibit an altered response to TGF-β. *J Invest Dermatol* 99:650–655, 1992

Backer JM, Myers MG, Shoelson SE, *et al*: Phosphatidylinositol 3-kinase is activated by association with IRS-1 during insulin stimulation. *EMBO J* 11:3469–3479, 1992

Border WA, Noble NA: Transforming growth factor beta in tissue fibrosis. *N Engl J Med* 331:1286–1292, 1994

Chin GS, Liu W, Peled Z, *et al*: Differential expression of transforming growth factor-beta receptors I and II and activation of Smad 3 in keloid fibroblasts. *Plast Reconstr Surg* 108:423–429, 2001

Chodon T, Sugihara T, Igawa HH, *et al*: Keloid-derived fibroblasts are refractory to Fas-mediated apoptosis and neutralization of autocrine transforming growth factor-beta1 can abrogate this resistance. *Am J Pathol* 157:1661–1669, 2000

Dennler S, Itoh S, Vivien D, Dijke Part Huet S, Gauthier JM: Direct binding of Smad3 and Smad4 to critical TGF-β -inducible elements in the promoter of human plasminogen activator inhibitor-type 1 gene. *EMBO J* 17:3091–3100, 1998

Derynck R, Zhang Y, Feng XH: Smad: Transcriptional activators of TGF-β responses. *Cell* 95:737–740, 1998

Finlay GA, Thannickal VJ, Fanburg BL, *et al*: Transforming growth factor-beta 1-induced activation of the ERK pathway/activator protein-1 in human lung fibroblasts requires the autocrine induction of basic fibroblast growth factor. *J Biol Chem* 275:27650–27656, 2000

Frey RS, Mulder KM: Involvement of extracellular signal-regulated kinase 2 and stress-activated protein kinase/jun N-terminal kinase activation by transforming growth factor beta in the negative growth control of breast cancer cells. *Cancer Res* 57:628–633, 1997

Ghahary A, Tredget EE, Shen Q, *et al*: Mannose-6-phosphate/IGF-II receptors mediate the effects of IGF-1-induced latent transforming growth factor beta 1 on expression of type I collagen and collagenase in dermal fibroblasts. *Growth Factors* 17:167–176, 2000

Gupta S, Campbell D, Derijard B, Davis RJ: Transcription factor ATF-2 regulation by the JNK signal transduction pathway. *Science* 267:389–393, 1995

Hanafusa HE, Ninomiya TJ, Masuyama N, *et al*: Involvement of the p38 mitogen-activated protein kinase pathway in transforming growth factor-beta-induced gene expression. *J Biol Chem* 274:27161–27167, 1999

Heldin CH, Miyazono K, Dijke P: TGF-β signaling from cell membrane to nucleus through Smad proteins. *Nature* 390:465–471, 1997

Huang HC, Murtaugh LC, Vizw PD, Whitman M: Identification of a potential regulator of early transcriptional responses to mesoderm inducers in the frog embryo. *EMBO J* 14:5965–5973, 1995

Ishihara H, Yoshimoto H, Fujioka M, *et al*: Keloid fibroblasts resist ceramide-induced apoptosis by overexpression of insulin-like growth factor I receptor. *J Invest Dermatol* 115:1065–1071, 2000

Kara CJ, Liou HC, Ivashkiv LB, Glimcher LH: A cDNA for a human cyclic AMP response element-binding protein is distinct from CREB and expressed preferentially in brain. *Mol Cell Biol* 10:1347–1357, 1990

Ohtsuru A, Yoshimoto H, Ishihara H, *et al*: Insulin-like growth factor-I (IGF-I)/IGF-I receptor axis and increased invasion activity of fibroblasts in keloid. *Endocr J* 47 (Suppl.):S41–S44, 2000

Pena TL, Chen SH, Konieczny SF, Rane SG: Ras/MEK/ERK up-regulation of the fibroblast KCa channel FIK is a common mechanism for basic fibroblast growth factor and transforming growth factor-beta suppression of myogenesis. *J Biol Chem* 275 (18):13677–13682, 2000

Ravanti L, Toriseva M, Penttinen R, *et al*: Expression of human collagenase-3 (MMP-13) by fetal skin fibroblasts is induced by transforming growth factor beta via p38 mitogen-activated protein kinase. *FASEB J* 15:1098–1100, 2001

Roberts AB, Piek E, Bottinger EP, *et al*: Is Smad3 a major player in signal transduction pathways leading to fibrogenesis? *Chest* 120 (Suppl.1):43S–47S, 2001

Rogounovitch TI, Saenko VA, Shimizu-Yoshida Y, *et al*: Large deletions in mitochondrial DNA in radiation-associated human thyroid tumors. *Cancer Res* 62:7031–7041, 2002

Rozakis-Adcock M, Fernley R, Wade J, Pawson T, Bowtell D: The SH2 and SH3 domains of mammalian Grb2 couple the EGF receptor to the Ras activator mSos1. *Nature* 363:83–85, 1993

Sato M, Shegogue D, Gore EA, *et al*: Role of p38 MAPK in transforming growth factor beta stimulation of collagen production by scleroderma and healthy dermal fibroblasts. *J Invest Dermatol* 118:704–711, 2002

Skolnik EY, Lee CH, Batzer A, *et al*: The SH2/SH3 domain-containing protein GRB2 interacts with IRS1 and Shc: implications for insulin control of Ras-signaling. *EMBO J* 12:1929–1936, 1993

Tuan TL, Nichter LS: The molecular basis of keloid and hypertrophic scar formation. *Mol Med Today* 4:19–24, 1998

Ullrich A, Schlessinger J: Signal transduction by receptors with tyrosine kinase activity. *Cell* 61:203–212, 1990

Verrecchia F, Mauviel A: Transforming growth factor-beta signaling through the Smad pathway: role in extracellular matrix gene expression and regulation. *J Invest Dermatol* 118:211–215, 2002

Yingling JM, Datto MB, Wong C, Frederick JP, Liberati NT, Wang XF: Tumor suppressor Smad4 is a transforming growth factor beta-inducible DNA binding protein. *Mol Cell Biol* 17:7019–7028, 1997

Yoshimoto H, Ishihara H, Ohtsuru A, *et al*: Overexpression of insulin-like growth factor-1 (IGF-I) receptor and the invasiveness of cultured keloid fibroblasts. *Am J Pathol* 154:883–889, 1999

Younai S, Nichter LS, Wellisz T, *et al*: Modulation of collagen synthesis by transforming growth factor-beta in keloid and hypertrophic scar fibroblasts. *Ann Plast Surg* 33:148–151, 1994

Zawel L, Dai JL, Buckhaults P, Zhou S, Kinzlwe KW, Vogelstein B, Kern SE: Human Smad3 and Smad4 are sequence-specific transcription activators. *Mol Cell* 1:611–617, 1998

Zhou S, Zawel L, Lengauer C, Kinzler KW, Vogelstein B: Characterization of human FAST-1, a TGF beta and activin signal transducer. *Mol Cell* 2: 121–127, 1998

BRIEF OBSERVATION

Low Plasma Ghrelin Levels in Patients with *Helicobacter pylori*–Associated Gastritis

Hajime Isomoto, MD, Masamitsu Nakazato, MD, PhD, Hiroaki Ueno, MD, PhD, Yukari Date, MD, PhD, Yoshito Nishi, MD, Hiroshi Mukae, MD, PhD, Yohei Mizuta, MD, Akira Ohtsuru, MD, PhD, Shunichi Yamashita, MD, PhD, Shigeru Kohno, MD, PhD

Most cases of chronic gastritis are due to *Helicobacter pylori* infection (1). However, the severity and extent of *H. pylori*–associated chronic gastritis varies among infected patients. Those with pangastritis or corpus-predominant gastritis may develop progressive atrophy with loss of pyloric and oxyntic glands (2).

The stomach is the main source of ghrelin, a 28–amino acid peptide that is an endogenous ligand for the growth hormone secretagogue receptor (3,4). Ghrelin influences appetite, growth hormone secretion, energy balance, gastric motility, and acid secretion. It is produced by X/A-like cells in oxyntic glands in the stomach.

There are contradictory reports on the relation between *H. pylori* and ghrelin; a Turkish study reported that *H. pylori* infection had no effect on plasma ghrelin levels (5), whereas a British study demonstrated an increase in circulating ghrelin levels following cure of *H. pylori* (6). We speculated that the production and release of ghrelin are affected by inflammatory and atrophic events associated with *H. pylori*, and assessed the correlation of ghrelin levels with histologic severity and topographic extent of *H. pylori*–associated chronic gastritis.

METHODS

We enrolled consecutive outpatients between the ages of 18 and 80 years who had been referred for upper gastrointestinal endoscopy between April 2002 and March 2003. All patients provided written informed consent. We excluded those with any of the following: pregnancy, body mass index >30 kg/m^2, diabetes mellitus, cachexia (cancer, systemic infection, thyroid and liver diseases), renal impairment, peptic ulcer, use of medications effective against *H. pylori* during the preceding 3 months, alcohol abuse, drug addiction, and chronic corticosteroid or nonsteroidal anti-inflammatory drug use. None of the subjects had undergone gastrointestinal surgery.

Blood was taken between 8:00 AM and 10:00 AM after an overnight fast, transferred into chilled tubes containing ethylenediaminetetraacetic acid-2Na and aprotinin, and stored on ice during collection and centrifuged. Plasma was separated and stored at −80°C until assay. Ghrelin levels were measured in house in duplicate by radioimmunoassay (4). This assay system employs a rabbit polyclonal antibody raised against the C-terminal fragment [13–28] of human ghrelin, and can measure both the acylated and des-acyl forms. The intra-assay coefficient of variation was 2.8%; the inter-assay coefficient of variation was 3.1%. The minimum detection level was 10 fmol per tube. Plasma gastrin, leptin, and pepsinogen levels were determined by commercial radioimmunoassay kits. Serum samples were examined for anti–*H. pylori* immunoglobulin G antibodies by an enzyme-linked immunosorbent assay.

During endoscopy, two pairs of biopsy specimens were obtained from the antrum and corpus for histopathologic assessment of gastritis and presence of *H. pylori*. Biopsy specimens were fixed in 10% formalin and embedded in paraffin. The sections (4-μm thick) were deparaffinized, rehydrated, and stained with hematoxylin and eosin. Giemsa staining was used to detect *H. pylori*. According to the Sydney system, each histologic parameter of activity (neutrophils), chronic inflammation (mononuclear cells), glandular atrophy, and intestinal metaplasia was graded as none, mild, moderate, or severe (1). Topographic distribution of gastritis was designated as antrum predominant, pangastritis, or corpus predominant (2). Biopsy specimens were examined blindly without knowledge of ghrelin levels.

We treated 12 *H. pylori*–positive patients with a 7-day course of triple therapy consisting of lansoprazole, amoxicillin, and clarithromycin (7). Four weeks after cessation of treatment, fasting plasma ghrelin levels were measured. Eradication of *H. pylori* was considered successful when the ^{13}C-urea breath test was negative (7).

Statistical Analysis

Statistical analyses were performed using the Fisher exact test, the chi-squared test, the Student *t* test, the Mann-Whitney *U* test, the Kruskal-Wallis test, or analysis of variance, as appropriate. A *P* value of less than 0.05 was accepted as statistically significant. The study was approved by the Nagasaki University Ethics Committee.

RESULTS

We studied 68 patients (mean [± SD] age, 56 ± 14 years; range, 20 to 80 years), including 35 women. Eighteen were current smokers and 16 drank alcohol. Based on histopathology and serology, 43 patients were designated as positive for *H. pylori* infection. The mean plasma

0002-9343/04/$–see front matter
doi:10.1016/j.amjmed.2004.01.030

Table. Plasma Ghrelin Levels and Histologic Severity of Each Parameter of Gastritis

Parameter	Severity of Gastritis				*P* Value
	None	Mild	Moderate	Severe	
	Mean (± SD) Ghrelin Level in fmol/mL (No. of Subjects)				
Activity					
Antrum	179 ± 87 (33)	75 ± 8 (18)	117 ± 48 (12)	102 ± 52 (5)	<0.001
Corpus	177 ± 86 (23)	123 ± 48 (16)	85 ± 30 (24)	98 ± 34 (5)	<0.001
Chronic inflammation					
Antrum	146 ± 84 (33)	105 ± 46 (24)	106 ± 43 (8)	121 ± 105 (3)	0.15
Corpus	152 ± 81 (33)	95 ± 41 (18)	95 ± 35 (12)	86 ± 20 (5)	<0.05
Glandular atrophy					
Antrum	166 ± 85 (27)	115 ± 48 (21)	79 ± 28 (13)	85 ± 53 (7)	<0.0001
Corpus	168 ± 74 (34)	93 ± 21 (12)	78 ± 16 (17)	59 ± 12 (5)	<0.0001
Intestinal metaplasia					
Antrum	143 ± 77 (44)	107 ± 57 (11)	78 ± 41 (7)	93 ± 42 (6)	0.07
Corpus	134 ± 73 (56)	No data	78 ± 16 (8)	63 ± 15 (4)	<0.05

ghrelin level was 127 ± 88 fmol/mL (range, 42 to 584 fmol/mL). Baseline characteristics, including age, sex, alcohol intake, smoking habits, body mass index, and biochemical markers, were not associated with ghrelin levels. However, the mean ghrelin level in *H. pylori*–positive patients (99 ± 44 fmol/mL) was significantly lower than in *H. pylori*–negative patients (175 ±119 fmol/mL, $P < 0.001$).

There were also significant differences in ghrelin levels based on the grades of each histopathologic parameter: activity in the antrum and corpus, chronic inflammation in the corpus, glandular atrophy in the antrum and corpus, and intestinal metaplasia in the corpus (Table). There was a stepwise decrease in ghrelin levels from normal to the antrum-predominant pattern to pangastritis to corpus-predominant gastritis (Figure 1).

Plasma ghrelin levels correlated significantly with pepsinogen I levels and pepsinogen I/II ratios (Figure 2), but not with pepsinogen II ($r = 0.15$, $P = 0.22$) or gastrin ($r = 0.09$, $P = 0.47$) levels.

Within the *H. pylori*–positive group, there was a negative correlation between age and ghrelin levels ($r = -0.31$, $P < 0.05$). In comparison, ghrelin levels did not correlate with age in *H. pylori*–negative patients ($r = 0.07$, $P = 0.74$). There was a negative correlation between age and pepsinogen I/II ratios ($r = -0.30$, $P < 0.05$) in *H. pylori*–positive patients.

H. pylori infection was cured in 9 of the 12 patients who received eradication therapy. There was no significant difference in plasma ghrelin levels measured before and after treatment (Figure 3).

DISCUSSION

We found that plasma ghrelin levels were significantly lower in *H. pylori*–positive than in *H. pylori*–negative patients. The results contrast with those from a previous study that reported no effect of *H. pylori* infection on ghrelin levels (5). There are several possible explanations for this disparity, including differences in the radioimmunoassay protocols for ghrelin; differences in the assessment of *H. pylori* status (the prior study used histol-

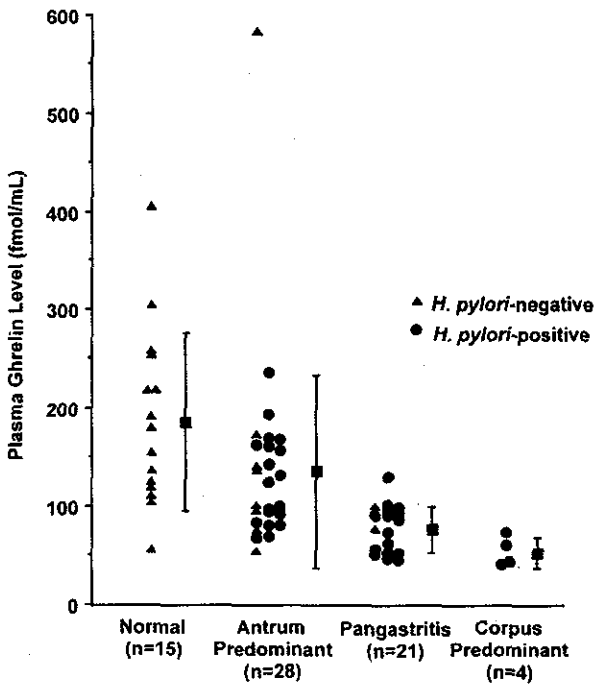

Fig. 1. Relation between topographic distribution of chronic gastritis, *Helicobacter pylori* infection, and plasma ghrelin levels. Mean (± SD) ghrelin levels were 190 ± 90 fmol/mL in those with normal mucosa without *H. pylori* infection, 139 ± 98 fmol/mL in those with antrum-predominant gastritis, 80 ± 24 fmol/mL in those with pangastritis, and 56 ± 15 fmol/mL in those with corpus-predominant gastritis ($P < 0.0001$).

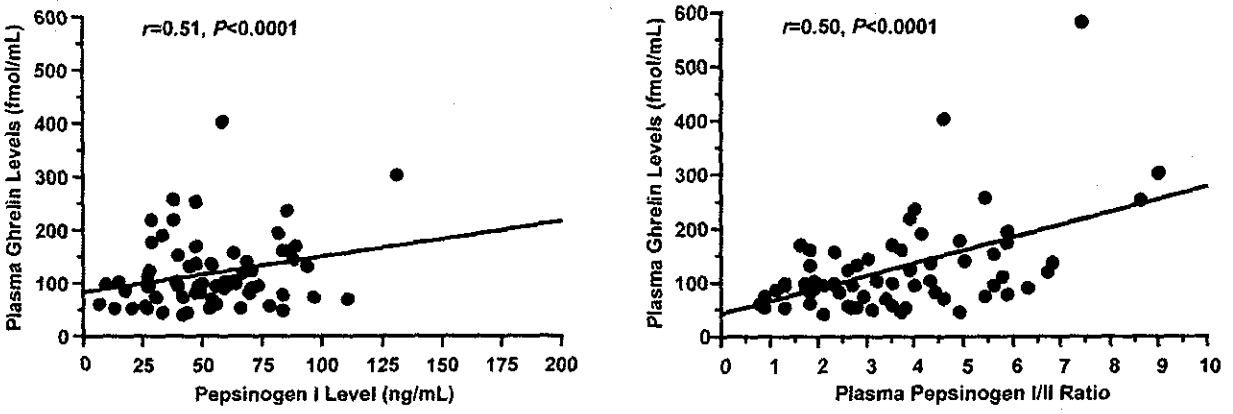

Fig. 2. Correlations between plasma ghrelin and pepsinogen I levels (left) and pepsinogen I/II ratio (right).

ogy only, thereby underestimating infection); differences in the samples with respect to race, nutrient status, and dietary habits; and small sample size (8).

Although gastrin may modify the production or release of ghrelin (9), we found no significant correlation between plasma ghrelin and gastrin levels, irrespective of *H. pylori* status. Consistent with our findings, recent observations demonstrated that ghrelin administration does not affect circulating gastrin levels in humans (10). In addition, increased levels of gastrin caused by omeprazole treatment failed to raise either the level of ghrelin messenger RNA in oxyntic mucosa or circulating ghrelin levels in a rat model (11). Based on these findings, ghrelin production or release does not seem to be controlled by gastrin.

The major finding of our study was that the severity of histopathologic changes and topography of gastritis affected circulating ghrelin levels, which were decreased markedly in patients with extensive atrophic gastritis involving the corpus. The reduced plasma ghrelin levels were accompanied by decreased pepsinogen I levels and low pepsinogen I/II ratios, which are thought to be markers of gastric mucosal atrophy (2). Indeed, a low plasma ghrelin level has been observed in a young woman with an evolving autoimmune gastric process, including serum anti–parietal cell antibodies and a low B_{12} level (12). Given the close juxtaposition of the endocrine and parietal cell compartments, ghrelin biosynthesis in fundic mucosa may be affected by inflammatory and atrophic events associated with either *H. pylori* infection or an autoimmune reaction. This may explain the progressive fall in circulating ghrelin levels with increased severity and extent of gastritis that we observed, probably reflecting the loss of ghrelin-producing cells.

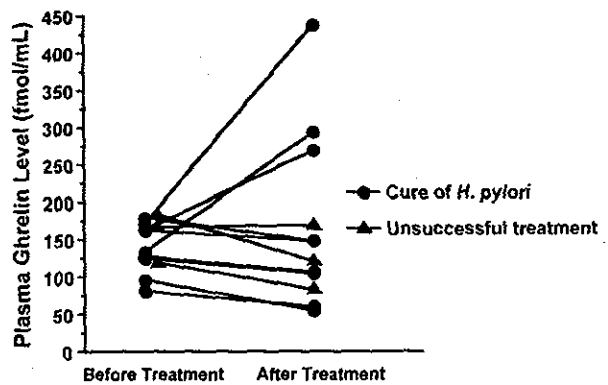

Fig. 3. Plasma ghrelin levels before and after 7-day triple eradication treatment against *Helicobacter pylori* infection. Mean (± SD) ghrelin levels were 142 ± 33 fmol/mL before treatment and 166 ± 113 fmol/mL after treatment.

However, Nwokolo et al (6) reported that 6-hour integrated plasma ghrelin levels increased substantially following cure of *H. pylori* infection, suggesting that depressed ghrelin levels in *H. pylori* infection were caused in part by a functional impairment due to inflammation, rather than loss of ghrelin-producing cells. We did not observe a rise in plasma ghrelin levels after cure of *H. pylori* infection, although we measured levels at only one point after an overnight fast. Study of a large number of patients with placebo controls is warranted to elucidate the reversibility of ghrelin production after cure of *H. pylori* infection.

We observed a significant negative correlation between age and circulating ghrelin levels in *H. pylori*–infected patients, perhaps reflecting progressive atrophic gastritis with greater years of infection. One other study reported lower plasma ghrelin levels in elderly persons (13). Since ghrelin levels did not correlate with age in *H. pylori*–negative patients, we believe that this age effect may be restricted to those infected with *H. pylori*.

Further characterization of the implications of low production or release of ghrelin on physiological functions is warranted. In particular, ghrelin deficiency could be viewed as an *H. pylori*–associated endocrine disorder (e.g., somatotroph dysregulation and anorexia of aging). The high plasma ghrelin levels in *H. pylori*–negative pa-

tients may affect appetite and food intake, and even contribute to increased obesity seen in developed countries where the prevalence of *H. pylori* infection is on the decline.

REFERENCES

1. Dixon MF, Genta RM, Yardley JH, et al. Classification and grading of gastritis. *Am J Surg Pathol.* 1996;20:1161–1181.
2. Bodger K, Wyatt JI, Heartley RV. Variation in serum pepsinogens with severity and topography of *Helicobacter pylori*-associated chronic gastritis in dyspeptic patients referred for endoscopy. *Helicobacter.* 2001;6:216–224.
3. Yoshihara F, Kojima M, Hosoda H, et al. Ghrelin: a novel peptide for growth hormone release and feeding regulation. *Curr Opin Clin Nutr Metab Care.* 2002;5:391–395.
4. Date Y, Kojima M, Hosoda H, et al. Ghrelin, a novel growth hormone-releasing acylated peptide, is synthesized in a distinct endocrine cell type in the gastrointestinal tracts of rats and humans. *Endocrinology.* 2000;141:4255–4261.
5. Gokcel A, Gumurdulu Y, Kayaselcuk F, et al. *Helicobacter pylori* has no effect on plasma ghrelin levels. *Eur J Endocrinol.* 2003;148:423–426.
6. Nwokolo CU, Freshwater DA, O"Hare P, Randeva HS. Plasma ghrelin following cure of *Helicobacter pylori*. *Gut.* 2003;52:637–640.
7. Isomoto H, Inoue K, Furusu H, et al. Lafutidine, a novel histamine H_2-receptor antagonist, vs lansoprazole in combination with amoxicillin and clarithromycin for eradication of *Helicobacter pylori*. *Helicobacter.* 2003;8:111–119.
8. Isomoto H, Mizuta Y, Inoue K, et al. A close relationship between *Helicobacter pylori* infection and gastric xanthoma. *Scand J Gastroenterol.* 1999;34:346–352.
9. Lee HM, Wang G, Englander EW, et al. Ghrelin, a new gastrointestinal endocrine peptide that stimulates insulin secretion: enteric distribution, ontogeny, influence of endocrine, and dietary manipulations. *Endocrinology.* 2002;143:185–190.
10. Arosio M, Ronchi CL, Cebbia C, et al. Stimulatory effects of ghrelin on circulating somatostatin and pancreatic polypeptide levels. *J Clin Endocrinol Metab.* 2003;88:701–704.
11. Dornonville de la Cour C, Bjorkqvist M, Sandvik AK, et al. A-like cells in the rat stomach contain ghrelin and do not operate under gastrin control. *Regul Pept.* 2001;99:141–150.
12. Cummings DE, Purnell JQ, Frayo RS, et al. A preprandial rise in plasma ghrelin levels suggests a role in meal initiation in humans. *Diabetes.* 2001;50:1714–1719.
13. Rigamonti AE, Pincelli AI, Corra B, et al. Plasma ghrelin concentrations in elderly subjects: comparison with anorexic and obese patients. *J Endocrinol.* 2002;175:R1–R5.

From the Second Department of Internal Medicine (HI, YN, HM, YM, SK), and Department of Molecular Medicine, Atomic Bomb Disease Institute (AO, SY), Nagasaki University School of Medicine, Nagasaki, Japan; and Third Department of Internal Medicine (MN, HU, YD), Miyazaki Medical College, Miyazaki, Japan.

Requests for reprints should be addressed to Hajime Isomoto, MD, Gastrointestinal Unit, Massachusetts General Hospital, Jackson 706, 55 Fruit Street, Boston, Massachusetts 02114-2696, or hajimei2002@yahoo.co.jp.

Manuscript submitted June 30, 2003, and accepted in revised form January 29, 2004.

ELSEVIER

Molecular and Cellular Endocrinology 218 (2004) 137–146

MCE
Molecular and Cellular Endocrinology

www.elsevier.com/locate/mce

GH suppresses TGF-β-mediated fibrosis and retains cardiac diastolic function

Ryo Imanishi [a], Naoto Ashizawa [a,*], Akira Ohtsuru [b], Shinji Seto [a], Yuri Akiyama-Uchida [a], Hiroaki Kawano [a], Hiroaki Kuroda [b], Masahiro Nakashima [c], Vladimir A. Saenko [b], Shunichi Yamashita [b], Katsusuke Yano [a]

[a] *Department of Cardiovascular Medicine, Course of Medical and Dental Sciences, Graduate School of Biomedical Sciences, Nagasaki University, 1-7-1 Sakamoto, Nagasaki 852-8501, Japan*

[b] *Department of Molecular Medicine, Atomic Bomb Disease Institute, Graduate School of Biomedical Sciences, Nagasaki University, 1-12-4 Sakamoto, Nagasaki 852-8523, Japan*

[c] *Department of Molecular Pathology, Atomic Bomb Disease Institute, Graduate School of Biomedical Sciences, Nagasaki University, 1-12-4 Sakamoto, Nagasaki 852-8523, Japan*

Received 3 December 2003; received in revised form 3 December 2003; accepted 4 December 2003

Abstract

The aims of this study were to elucidate the molecular mechanism by which growth hormone (GH) excess is anti-fibrotic in vitro and in vivo model. The in vivo model GH excess showed a significant increase of relative wall thickness with no concomitant disturbance of cardiac diastolic function. Western blot for extracellular matrix (ECM) structural proteins showed minimal change in the GH treatment group, compared to an Angiotensin II (Ang II) subpressor dose group. In cultured cardiac fibroblasts, we investigated the abundance of ECM proteins, phosphorylation of p38 mitogen-activated protein kinase (MAPK), and transforming growth factor-β (TGF-β)-specific transcriptional activity. GH down-regulated the expression of PAI-1 and fibronectin proteins activated by TGF-β. In reporter assays, GH, but not insulin-like growth factor-1 (IGF-1), reduced TGF-β-specific transcriptional activity. Moreover, GH markedly down-regulated TGF-β-induced phosphorylation of p38 MAPK. These results demonstrated that a chronic excess of GH have an anti-fibrotic effect on cardiac remodeling, probably through a down-regulation of TGF-β signaling via de-phosphorylation of p38 MAPK.

Keywords: Growth hormone; Diastolic dysfunction; TGF-β; Fibrosis; Extracellular matrix

1. Introduction

Growth hormone (GH) and its local effectors, e.g. insulin-like growth factor-1 (IGF-1) have been shown to be essential for cardiac development and for maintaining cardiac mass and performance (Sacca et al., 1994). In previous studies, It was reported that chronic (4 weeks) exogenous administration of GH and IGF-1 in normal rats induced a cardiac hypertrophic response without disturbance of diastolic function and significant fibrosis (Cittadini et al., 1996). GH therapy for three months in an uncontrolled trial of seven adult patients with idiopathic dilated cardiomyopathy caused a significant increase in left ventricular (LV) mass and an improvement of hemodynamics (Fazio et al., 1996). Experimentally in the setting of post-infarction heart failure, reactivation of myocardial growth using GH therapy has consistently been shown to be beneficial (Cittadini et al., 1997, Duerr et al., 1995, Yang et al., 1995), and GH therapy, given early after large myocardial infarction, elicited a unique pattern of structural effects characterized by reduced adaptive fibrosis (Grimm et al., 1998). On the other hand, chronic GH and IGF-1 excess caused a specific derangement of cardiomyocytes (Lopez-Velasco et al., 1997, Rodrigues et al., 1989) with an increased incidence of myocyte apoptosis (Frustaci et al., 1999). There was a significant increase in LV mass in fifty adult patients with dilated cardiomyopathy given a randomized, placebo-controlled study of recombinant human GH, but this was not accompanied by improvements in ejection fraction and clinical status (Osterziel et al., 1998). Also,

* Corresponding author. Tel.: +81-95-849-7288; fax: +81-95-849-7290.
E-mail address: r-ima@net.nagasaki-u.ac.jp (N. Ashizawa).

0303-7207/$ – see front matter © 2003 Elsevier Ireland Ltd. All rights reserved.
doi:10.1016/j.mce.2003.12.004

patients with acromegaly have been shown to experience cardiac complications including biventricular hypertrophy, impaired diastolic filling and decreased cardiac performance during exercise, due to diastolic and systolic dysfunction (Morvan et al., 1991). Based on recent studies, acromegaly in its early stage (<5 years) showed evidence of LV hypertrophy and no alteration of diastolic function (Fazio et al., 2000). However, after a long-term exposure to GH, the developing interstitial fibrosis in the myocardium gradually impairs diastolic function (Clayton, 2003). Therefore, elucidation of molecular mechanisms of anti-fibrotic effect of GH is necessary to reduce the side effects of long term GH therapy.

In general, disproportional accumulation of fibrous tissue is a major determinant of pumping capacity in hypertrophied hearts, and accounts for a spectrum of ventricular diastolic dysfunction. Several studies in humans and in experimental models have shown that there was an increase in myocardial transforming growth factor-β (TGF-β) expression during cardiac hypertrophy (Schultz et al., 2002, Takahashi et al., 1994, Tomita et al., 1998). TGF-β has been found to stimulate the expression of fibronectin and collagen and their incorporation into the extracellular matrix (ECM) in cardiac fibroblasts (Eghbali et al., 1991, Ignotz and Massague, 1986, Sigel et al., 1996). In a recent study, inhibition of TGF-β using neutralizing antibodies prevented progression of diastolic dysfunction and myocardial fibrosis in a cardiac model of pressure-overload (Kuwahara et al., 2002).

Although a number of studies have looked at the effects of GH therapy, reported changes in cardiac function and pathological remodeling evoked by the GH excess are controversial, and there is little information as to the TGF-β-mediated molecular mechanism by which GH excess retains cardiac diastolic function despite the development of cardiac hypertrophy. In the present study, we have examined the hypothesis that a chronic excess of GH in the normal rat has a beneficial effect on cardiac morphology and function via an anti-fibrotic action. Furthermore, we have attempted to elucidate the molecular mechanism by which GH exerts an anti-fibrotic effect by focusing on the regulation of the TGF-β signaling pathway in cardiac fibroblasts.

2. Methods

2.1. Animal model

Four weeks old female Wistar-Furth rats weighing 80–100 g (Charles River Laboratories Inc., Osaka, Japan) were kept at 21 ± 2 °C, 55 ± 10% relative humidity, in a light-controlled room (12 h light/12 h dark). Experiments were conducted under the guidelines of the Animal Research Committee of Nagasaki University. Rats were randomized into three groups: GH group ($n = 11$), Angiotensin II (Ang II) group ($n = 11$) and a control group ($n = 9$). Blood pressure (BP) was measured every week using the tail-cuff method. The GH excess model used rats with a transplantable GH-secreting pituitary tumor cell line, GH3. Using this model, Penney et al. observed a significant elevation of myocardial contractility and a high cardiac output (Penney et al., 1985). Ang II (Sigma Aldrich Chemie) was dissolved in saline at 4 mg/ml, and acetic acid (final concentration 0.01 mol/l) was added to maintain its stability. A subpressor dose of Ang II (150 ng/kg/min) was continuously administrated via a subcutaneous-implanted osmotic minipump (alzet model 2002, Alza Palo Alto, CA).

2.2. Echocardiography

After animals had been treated for 8 weeks, echocardiography was performed under ethanol anesthesia (50 mg/kg). A Toshiba Powervision 8000 equipped with a 7.5 MHz phased-array transducer was used. Anterior wall and posterior wall thickness (PWT) and LV internal dimensions were measured. Systolic function was assessed by calculating endocardial fractional shortening, and diastolic function was evaluated by early transmitral flow velocity/atrial flow velocity ratio (E/A ratio). Relative wall thickness was calculated as 2 × PWT/LV internal dimension (Cittadini et al., 1996). Two-dimensionally guided pulse doppler recordings of LV inflow were obtained from the apical four-chamber view.

2.3. Serum analysis

Blood samples were collected at the time of animal sacrifice. Serum was stored and frozen at −80 °C until the analysis. Rat GH was measured using ELISA and total serum IGF-1 was measured using radioimmunoassay, according to previously described methods (Albini et al., 1991, Lieberman et al., 1992).

2.4. Matrix metalloproteinase in situ zymography

Matrix metalloproteinase (MMP) activity was measured in cardiac tissue specimens using MMP and MMP-PT in situ zymography (Nakamura et al., 1999) (Wako Chemical). MMP Zymo-Film is composed of a layer of special processed gelatin, and MMP-PT contains a 1, 10-phenanthroline, specific MMP inhibitor, allowing to distinguish MMP activity from that of other proteinases. Briefly, frozen sections were made using a cryostat and mounted onto the gelatin surface of Zymo-Film. Specimens were then incubated in a humid chamber for 24 h at 37 °C. They were subsequently stained with Biebrich Scarlet solution and with Mayer's Hematoxylin solution.

2.5. Western blot analysis

Western blot analysis was performed according to the method (Akiyama et al., 1999) with minor modifications.

The primary antibodies used were against plasminogen activator inhibitor-1 (PAI-1) (American Diagnostics Inc.), fibronectin (Calbiochem), collagen types I and III (Rockland Immunochemicals), TGF-β1 (Santa Cruz Biotechonology), phospho- and total-p38 mitogen-activated protein kinase (MAPK) (Cell Signaling Technology), and β-actin (Santa Cruz Biotechnology). The proteins were detected using enhanced enzyme-linked chemiluminescence (Amersham).

2.6. Cell isolation and culture

Neonatal cardiac fibroblasts were prepared from Sprague–Dawley rats as described previously (Iwami et al., 1996). Briefly, cells were cultured in Dulbecco's Modified Eagle Medium (DMEM)/F12 nutrient mixture (DMEM/F12, 1:1) containing 10% fetal bovine serum. Cardiac fibroblasts were exposed to TGF-β (1 ng/ml, Sigma Aldrich Chemie), GH (100 ng/ml, Growject, Sumitomo Pharmacology), IGF-1 (100 ng/ml, Sigma Aldrich Chemie), and Ang II (10 nmol/l) for 30 min, 24 h or 48 h as previously described (Akiyama-Uchida et al., 2002, Ashizawa et al., 1996, Lu et al., 2001, Mehrhof et al., 2001).

2.7. DNA transfection and luciferase assay

A 3TP-Luciferase (Lux), activin response element (ARE)-Lux, and forkhead activin signal transducer-1 (FAST-1) expression vectors were used. 3TP-Lux is a TGF-β1-responsive luciferase reporter gene that contains three consecutive TPA response elements and a portion of the PAI-1 promoter region (Wrana et al., 1992). FAST-1 possesses the ability to bind to Smad2 and activates an ARE. ARE-Lux is used for the transcriptional activity of Smad signals. Cardiac fibroblasts, at 80% confluence, were transiently transfected with 1 μg of 3TP-Lux or ARE-Lux vectors. pRL-CMV *Renillla* luciferase was co-trasnfected as a control reporter vector. Twenty-four hours later, the medium was changed for a serum-free medium containing 10 mmol/l ascorbate (Sigma Aldrich Chemie) and 300 mmol/l pyruvate (Sigma Aldrich Chemie). Twenty-four hours after serum depletion, cells were treated with TGF-β, GH, IGF-1, IGF-binding protein 3 (IGF-BP3, 100 ng/ml, Sigma Aldrich Chemie), or Ang II for 24 h. Cells were harvested using a cell lysis buffer, and luciferase activity was assessed using a Dual-Luciferase™ Reporter Assay System (Promega).

2.8. Statistical analysis

Data are represented as mean ± S.E.M. One-way analysis of variance (ANOVA) followed by Scheffe's *F*-test was performed for the statistical comparisons. Differences were considered statistically significant when $P < 0.05$.

3. Results

3.1. Animal model and blood analysis

Body weight, heart, kidney and liver weights, and serum levels of GH, IGF-1 and BP were shown in Table 1. There was no significant difference in BP among the three groups. Body weight and heart weight were significantly greater in the GH group. Also, the ratio of heart weight to body weight was significantly increased in the GH group. The serum level of rat GH in the GH group was conspicuously higher than that in the control and Ang II groups. The GH group was also characterized by nearly two times higher level of blood IGF-1 concentration compared to the control group.

3.2. Echocardiography

Echocardiographic study was performed in the control, Ang II, and the GH group at 8-week treatment (Fig. 1). In the GH group, M-mode echocardiography detected a significantly increased LV wall thickness, whereas fractional shortening was similar to that in the Ang II and control groups. E/A ratio was significantly reduced in the Ang II group compared to values in the control group. Importantly, E/A ratio

Table 1
Animal characteristics and hormone determinations

	C ($n = 9$)	Ang II ($n = 11$)	GH ($n = 11$)
Body weight (g)	209 ± 16	196 ± 15	273 ± 15[a,b]
Heart weight (g)	0.85 ± 0.1	0.73 ± 0.1	1.13 ± 0.2[a,b]
HW/BW (mg/g)	3.88 ± 0.5	3.71 ± 0.3	4.31 ± 0.6[a,b]
KW/BW (mg/g)	3.71 ± 0.6	3.57 ± 0.8	3.95 ± 0.2
LW/BW (mg/g)	34.1 ± 3.5	35.5 ± 1.3	53.7 ± 3.1[a,b]
Serum GH (ng/ml)	18 ± 3	25 ± 10	4932 ± 2245[a,b]
Serum IGF-1 (ng/ml)	805 ± 43	816 ± 31	1544 ± 116[a,b]
Blood pressure (mmHg)	128 ± 11	135 ± 3	126 ± 8

Data are expressed as mean ± S.E.M. C indicates control group; Ang II, Angiotensin II-infused group; GH: growth hormone-treated group; BW: body weight; HW: heart weight; KW: kidney weight; LW: liver weight.

[a] $P < 0.05$ vs. control group.

[b] $P < 0.05$ vs. Ang II-infused group.

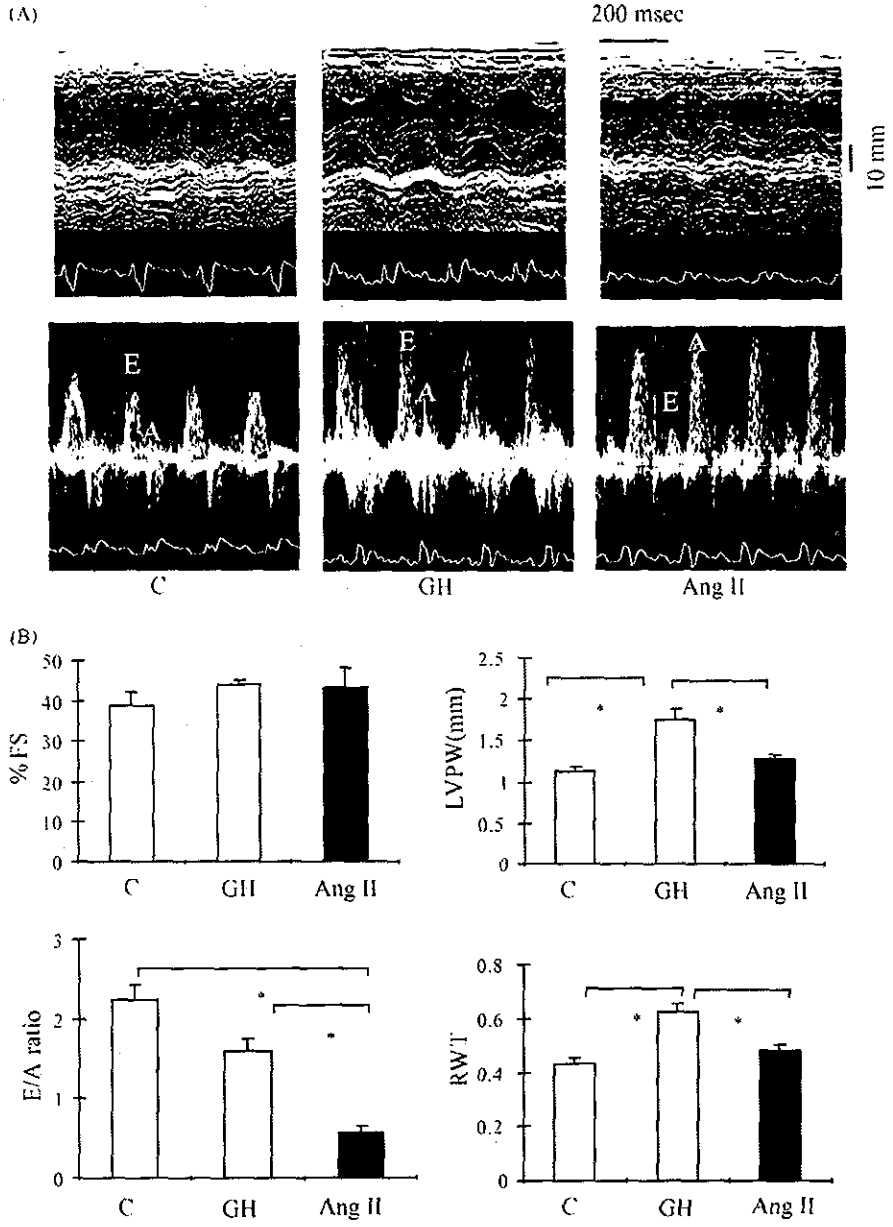

Fig. 1. Transthoracic echocardiographic findings in the three study groups. (A) Representative M-mode echocardiograms (top) and transmitral inflow Doppler patterns (bottom) after 8-week treatment. (B) FS (%) indicates fractional shortening; E/A ratio, early transmitral flow velocity/atrial flow velocity ratio; LVPW, left ventricular posterior wall; RWT, relative wall thickness; in control, GH and Ang II groups. Open bars represent control rats, gray bars represent GH-treated rats, and solid bars represent Ang II-infused rats. Data are expressed as mean ± S.E.M. RWT = 2× Posterior Wall/LV Diastolic dimension. * $P < 0.05$.

remained within the normal range in the GH group. Conversely, in the Ang II group, there was mild LV hypertrophy accompanied by LV diastolic dysfunction. The relative wall thickness was significantly increased in the GH group, suggesting the existence of concentric hypertrophy.

3.3. MMP activity

The results in Fig. 2 showed that there was no difference between the control and GH groups in terms of the MMP activity. However, it was significantly enhanced in the Ang II group as seen from the inhibitory studies using MMP-PT in situ Zymo-Film.

3.4. Expression of ECM proteins, TGF-β1 in heart tissue of each treatment

To examine whether ECM was enhanced in the GH group, Western blot analysis was performed. The expression of PAI-1 protein, as a marker of fibrosis caused by TGF-β,

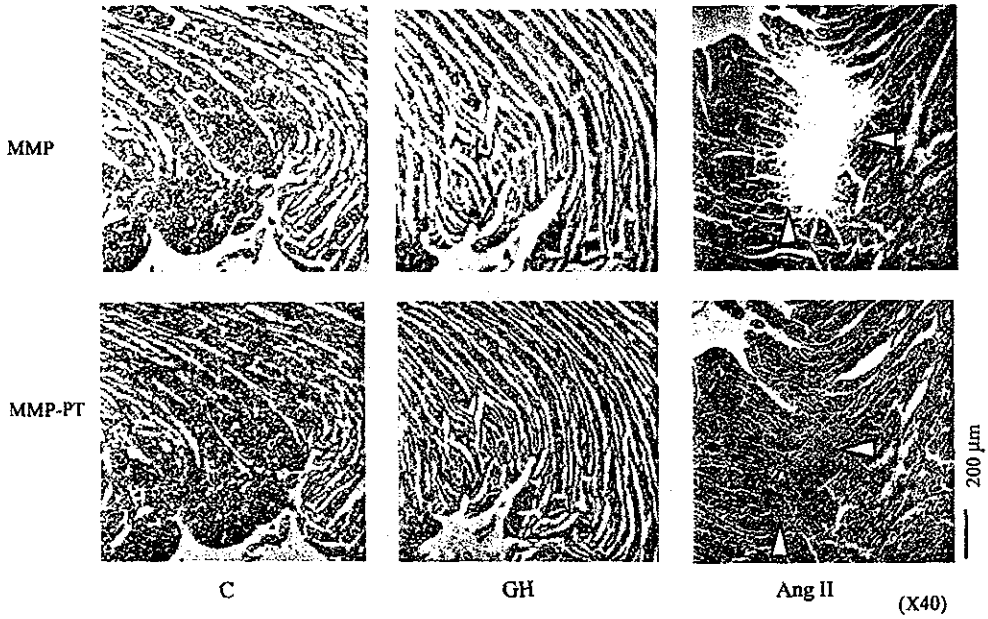

Fig. 2. MMP in situ zymographic analyses in the three study groups. To evaluate MMP activity, serial frozen sections were subjected to film MMP in situ zymography (top), and MMP-PT in situ zymography (bottom). Note the marked MMP activity in the Ang II group (arrows), whereas no activity was detected in the GH group.

was significantly increased in the Ang II group, whereas there was only a slight increase in the GH group compared with controls. Fibronectin, collagen type I, and collagen type III showed similar characteristics as PAI-1. In contrast, expression of TGF-β1 was significantly elevated in the GH group, and there was the strongest accumulation of these factors in the Ang II group as compared to controls (Fig. 3).

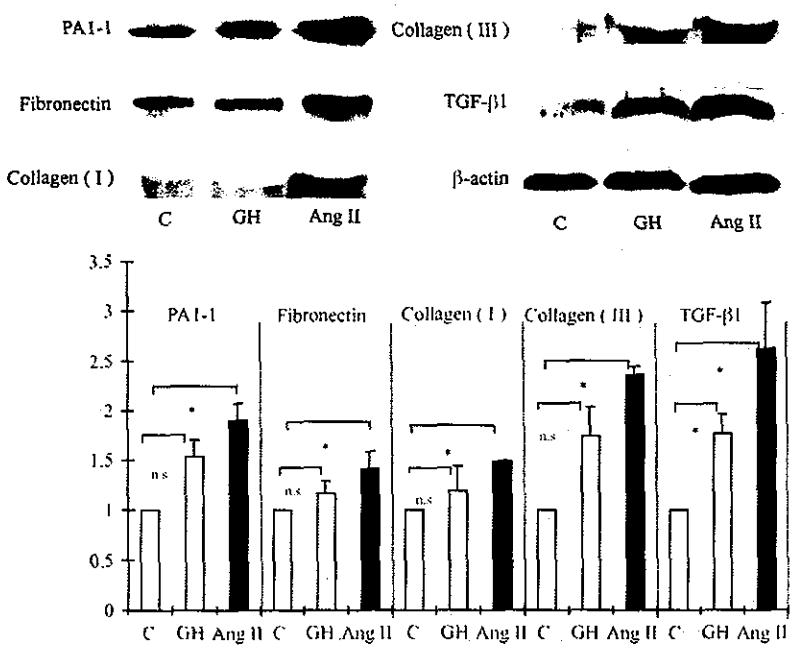

Fig. 3. Western blotting of ECM proteins, TGF-β1, and β-actin in homogenized heart tissue from each of the treatment groups. Results are expressed as fold increase compared with controls (mean ± S.E.M.). PAI-1, plasminogen activator inhibitor-1; TGF-β1, transforming growth factor-β1. $^{*}P < 0.05$; n.s., not significant.

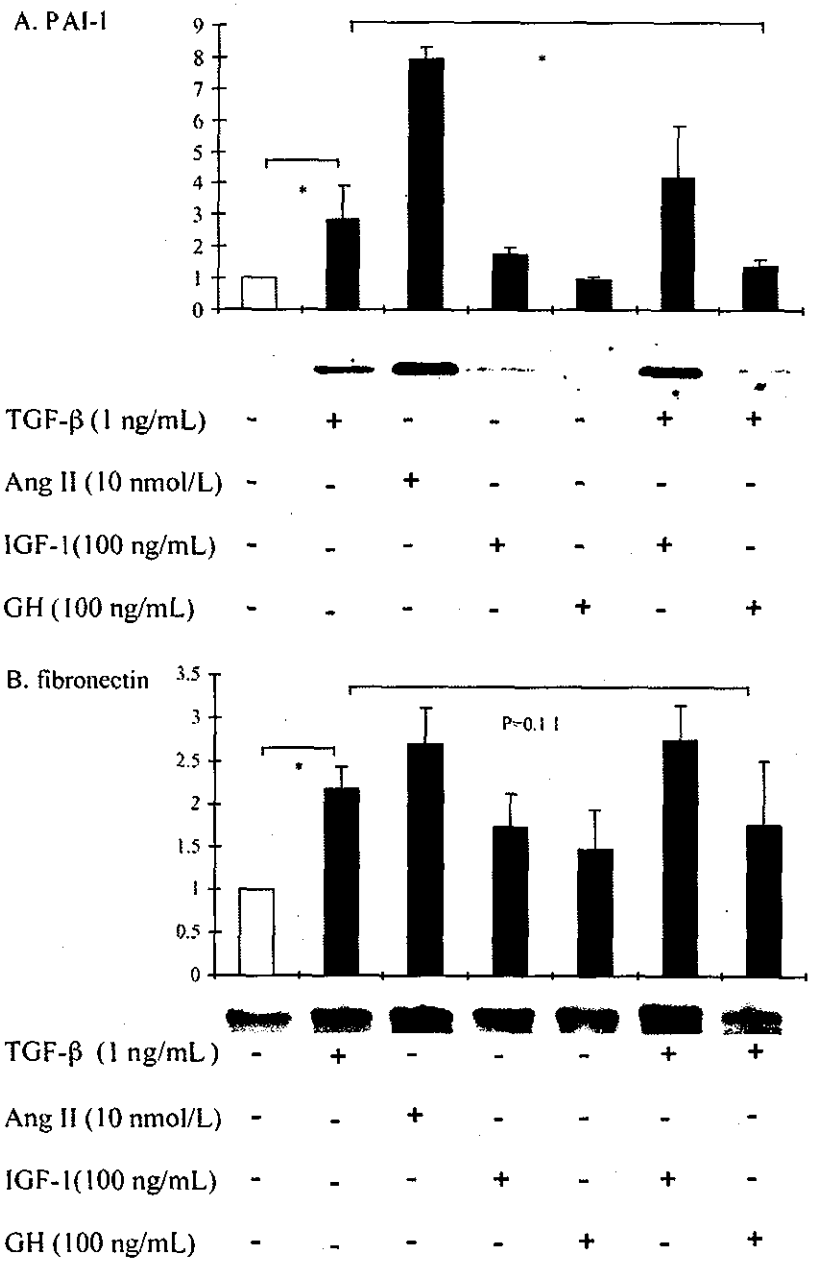

Fig. 4. Western blotting of extracts from cardiac fibroblasts. Cardiac fibroblasts were exposed to various stimuli for 48 h. The signal intensity for PAI-1 (A) and fibronectin (B) were evaluated by densitometric analysis. Results are expressed as fold increase compared with controls (mean ± S.E.M.). TGF-β, transforming growth factor-β; Ang II, Angiotensin II; IGF-1, insulin-like growth factor-1; GH, growth hormone; PAI-1, plasminogen activator inhibitor-1. $^{*}P < 0.05$.

3.5. Expression of ECM proteins in cultured cardiac fibroblasts

Fig. 4 showed representative Western blots of ECM components' expression in cultured cardiac fibroblasts. Expression of PAI-1 was markedly increased by treatment with TGF-β and Ang II. Treatment with GH or IGF-1 caused little to no changes compared with controls. The combination of IGF-1 and TGF-β caused up-regulation of PAI-1 expression compared with either IGF-1 or TGF-β treatment alone. In contrast, the combination of GH and TGF-β led to the significant attenuation of PAI-1 accumulation evoked by TGF-β (Fig. 4A). Similar results were obtained for fibronectin, although the difference between TGF-β and the combination of GH and TGF-β was not significant. (Fig. 4B).

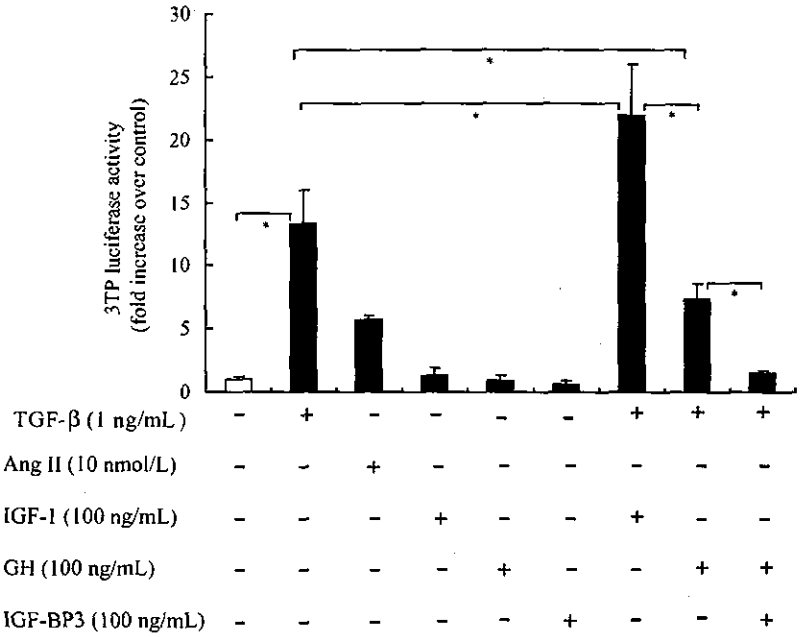

Fig. 5. 3TP-luciferase activity in cardiac fibroblasts. Cardiac fibroblasts were exposed to various stimuli for 24 h. Results are expressed as fold increase compared with controls (mean ± S.E.M.). TGF-β, transforming growth factor-β; Ang II, Angiotensin II; IGF-1, insulin-like growth factor-1; GH, growth hormone; IGF-BP3, insulin-like growth factor-binding protein 3. $^{*}P < 0.05$.

3.6. TGF-β signaling in cultured cardiac fibroblasts

As shown in Fig. 5, Ang II increased 3TP-Lux activity 5.7 ± 0.5-fold, whereas TGF-β treatment elevated it 13.1 ± 4.5-fold. IGF-1, GH, and IGF-BP3 treatment alone had no effect on 3TP-Lux activity (1.3 ± 0.6, 1.0 ± 0.3, and 0.7 ± 0.3-fold changes, respectively). Treatment with a combination of IGF-1 and TGF-β caused further increase in the reporter assay, whereas combination of GH and TGF-β decreased it compared to TGF-β alone. We next examined whether 3TP-Lux activity was suppressed when cardiac fibroblasts were treated with TGF-β, GH and IGF-1 specific inhibitor, IGF-BP3. In the presence of IGF-BP3, 3TP-Lux

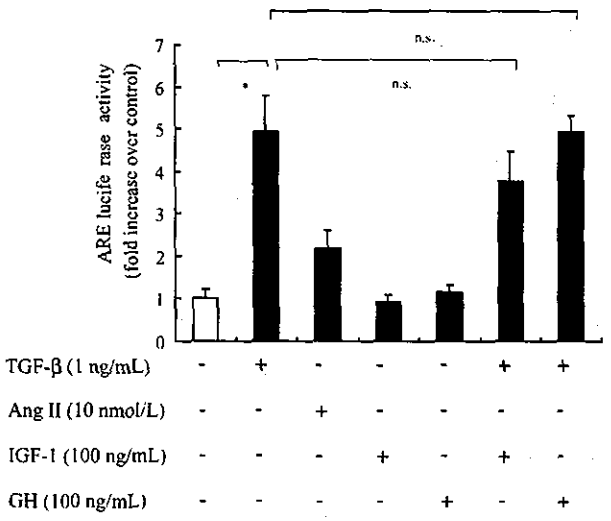

Fig. 6. ARE-luciferase activity in cardiac fibroblasts. Cardiac fibroblasts were exposed to various stimuli for 24 h. Results are expressed as fold increase compared with controls (mean ± S.E.M.). TGF-β, transforming growth factor-β; Ang II, Angiotensin II; IGF-1, insulin-like growth factor-1; GH, growth hormone. $^{*}P < 0.05$. n.s., not significant.

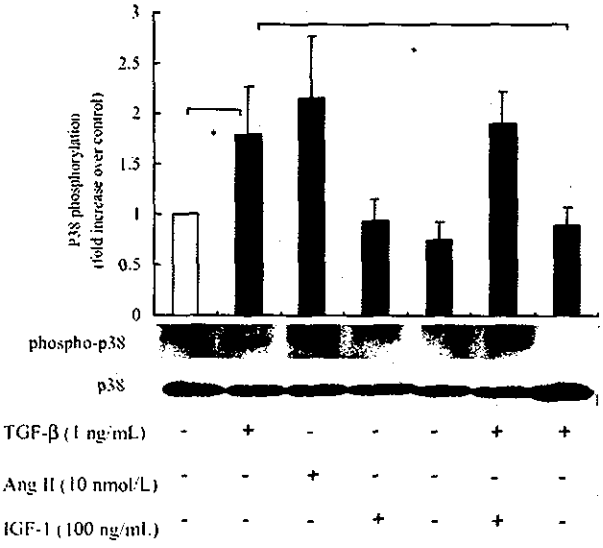

Fig. 7. Effect of various stimuli for 30 min after 24 h serum depletion on the level of active form of p38 MAPK in cardiac fibroblasts. Results are expressed as fold increase compared with controls (mean ± S.E.M.). TGF-β, transforming growth factor-β; Ang II, Angiotensin II; IGF-1, insulin-like growth factor-1; GH, growth hormone.

activity was further inhibited in cardiac fibroblasts treated with TGF-β and GH.

To determine whether effect of GH on TGF-β signaling is related to Smad cascades, we examined the ARE-Lux reporter system in the presence of FAST-1 upon various stimuli. ARE-Lux activity was not inhibited in cardiac fibroblasts treated with a combination of GH and TGF-β (Fig. 6).

In further studies, we examined whether TGF-β-induced phosphorylation of p38 MAPK was affected by the combination treatment with GH. TGF-β alone increased the level of phospho-p38 MAPK, whereas it was significantly suppressed when TGF-β was given in combination with GH (Fig. 7).

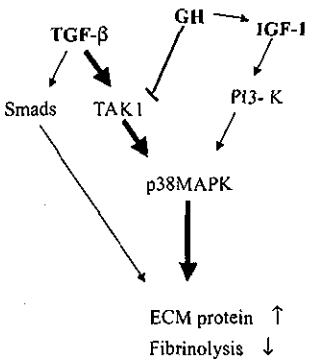

Fig. 8. A possible molecular mechanism of ECM production and fibrinolysis mediated by TGF-β, GH and IGF-1 cross-talk.

4. Discussion

In the present study, we first confirmed the effect of chronic high dose excess of GH on cardiac morphology and function in the normal rats. GH-treated rats showed marked cardiac hypertrophy without disturbance of cardiac function. In contrast, rats exposed to subpressor dose of Ang II had LV diastolic dysfunction coupled with mild cardiac hypertrophy. Consistent with these findings, Western blot for ECM accumulation was little different between the GH group and controls, and cardiac pericellular fibrosis was not increased in the GH group (data not shown). It was reported that following the administration of GH doses higher than 2 IU/kg per day for 4 weeks, effects on cardiac geometry and function became less favorable (Grimm et al., 1998). Apparently, differences in the therapeutic effects of subcutaneously administered recombinant GH and endogenously produced may account for a variant outcome of exposure to high dose excess of GH. In our studies, the tumor bearing animals with GH treatment for 8 weeks retained the cardiac geometry and function.

Major molecular pathways leading to cardiac fibrosis involve TGF-β signaling. In the GH group in our experiments, there was an up-regulated expression of TGF-β1 protein, whereas PAI-1, fibronectin, collagen type I and collagen type III expression remained little changed compared to controls. We, therefore, attempted to address the question as to why the GH group did not develop fibrosis in spite of an elevation of TGF-β with two possible explanations. First, ECM proteolysis might be specifically activated in the GH group. Second, the TGF-β signal transduction was nearly abolished by GH or IGF-1. As for the first assumption, we performed an in situ zymography to clarify whether matrix metalloproteinase activity was increased in the GH group. No induction of MMP activity was detected in the hearts from the GH group. Thus, GH may have an anti-fibrotic action via the suppression of TGF-β signal transduction on cardiac remodeling.

It is not clear whether the anti-fibrotic ventricular remodeling caused by GH is mediated via GH directly or through IGF-1 indirectly. Thus, we firstly performed experiments with cultured rat cardiac fibroblasts. To study production of the ECM proteins upon various stimuli, Western blot analysis demonstrated that IGF-1 in combination with TGF-β up-regulated expression of PAI-1 and fibronectin. In contrast, GH in combination with TGF-β restored expression values to control levels.

TGF-β binds to a heteromeric complex of Type I and Type II receptors and transmits signals via MAPK and signals via Smad pathways (Hoodless and Wrana, 1998). To elucidate the signaling mechanisms underlying the observed effects, we performed studies employing a TGF-β trans-acting reporter system. The 3TP-Lux activity was found to be markedly increased after treatment with IGF-1 and TGF-β, and significantly suppressed after treatment with GH and TGF-β. To clarify whether Smad cascades of TGF-β signaling were activated by GH, we examined the Smad signals using a reporter assay. Combination of GH and TGF-β did not down-regulate ARE-Lux activity in cardiac fibroblasts. Based on these results, we concluded the MAPKs cascade is involved in the determination of the GH effect on TGF-β signaling.

We have previously shown that norepinephrine and TGF-β had a synergistic effect on cardiac fibrosis which is mediated by p38 MAPK/ATF-2 pathway (Akiyama-Uchida et al., 2002). Also, IGF-1 enhances TGF-β-induced ECM protein production through the p38/ATF-2 signaling pathway in keloid fibroblast (Daian et al., 2003). We, therefore, addressed the question whether TGF-β-induced phosphorylation of p38 MAPK is affected by the combination treatment with GH and TGF-β in cardiac fibroblasts. Western blot analysis demonstrated that the level of TGF-β-induced phospho-p38 MAPK was decreased by treatment with GH. Fig. 8 shows a proposed molecular mechanism of the ECM production and fibrinolysis mediated by TGF-β, GH, and IGF-1 cross-talk. GH can interfere with TGF-β signaling via p38 MAPK de-phosphorylation, whereas IGF-1 and TGF-β costimulation leads to characteristic fibrosis and excess ECM production. Thus, GH may produce a dualistic effect on cardiac remodeling process. On one hand, it can suppress fibrotic changes, and on another, promote

them if the GH-IGF-1 pathway becomes prevalent in the micro-environment.

In conclusion, a chronic excess of GH in vivo induced concentric hypertrophy in an animal model with neither concomitant disturbance of cardiac function nor ECM accumulation observed. These effects appear to be due, in part, to a direct action of GH causing suppression of TGF-β signaling via de-phosphorylation of p38 MAPK. Further exploration of a therapeutic approach aimed at the down-regulation of TGF-β signaling may result in a novel promising treatment for advanced cardiac failure.

Acknowledgements

This work was supported by scientific grants-in-aid from the Japanese Ministry of Education, Science, and Culture (No. 14570677).

References

Akiyama, Y., Ashizawa, N., Seto, S., Ohtsuru, A., Kuroda, H., Ito, M., Yamashita, S., Yano, K., 1999. Involvement of receptor-type tyrosine kinase gene families in cardiac hypertrophy. J. Hypertens. 17, 1329–1337.

Akiyama-Uchida, Y., Ashizawa, N., Ohtsuru, A., Seto, S., Tsukazaki, T., Kikuchi, H., Yamashita, S., Yano, K., 2002. Norepinephrine enhances fibrosis mediated by TGF-β in cardiac fibroblasts. Hypertension 40, 148–154.

Albini, C.H., Sotos, J., Sherman, B., Johanson, A., Celniker, A., Hopwood, N., Quattrin, T., Mills, B.J., MacGillivray, M.H., 1991. Diagnostic significance of urinary growth hormone measurements in children with growth failure: correlation between serum and urine growth hormone. Pediatr. Res. 9, 619–622.

Ashizawa, N., Graf, K., Do, Y.S., Nunohiro, T., Giachelli, C.M., Meehan, W.P., Tuan, T.L., Hsueh, W.A., 1996. Osteopontin is produced by rat cardiac fibroblasts and mediates A(II)-induced DNA synthesis and collagen gel contraction. J. Clin. Invest. 98, 2218–2227.

Cittadini, A., Grossman, J.D., Napoli, R., Katz, S.E., Stromer, H., Smith, R.J., Clark, R., Morgan, J.P., Douglas, P.S., 1997. Growth hormone attenuates early left ventricular remodeling and improves cardiac function in rats with large myocardial infarction. J. Am. Coll. Cardiol. 29, 1109–1116.

Cittadini, A., Stromer, H., Katz, S.E., Clark, R., Moses, A.C., Morgan, J.P., Douglas, P.S., 1996. Differential cardiac effects of growth hormone and insulin-like growth factor-1 in the rat. A combined in vivo and in vitro evaluation. Circulation 93, 800–809.

Clayton, R.N., 2003. Cardiovascular function in acromegaly. Endocr. Rev. 24, 272–277.

Daian, T., Ohtsuru, A., Rogounovitch, T., Ishihara, H., Hirano, A., Akiyama-Uchida, Y., Saenko, V., Fujii, T., Yamashita, S., 2003. Insulin-like growth factor-I enhances transforming growth factor-β-induced extracellular matrix protein production through the P38/activating transcription factor-2 signaling pathway in keloid fibroblasts. J. Invest. Dermatol. 120, 956–962.

Duerr, R.L., Huang, S., Miraliakbar, H.R., Clark, R., Chien, K.R., Ross Jr., J., 1995. Insulin-like growth factor-1 enhances ventricular hypertrophy and function during the onset of experimental cardiac failure. J. Clin. Invest. 95, 619–627.

Eghbali, M., Tomek, R., Sukhatme, V.P., Woods, C., Bhambi, B., 1991. Differential effects of transforming growth factor-β1 and phorbol myristate acetate on cardiac fibroblasts. Regulation of fibrillar collagen mRNAs and expression of early transcription factors. Circ. Res. 69, 483–490.

Fazio, S., Cittadini, A., Biondi, B., Palmieri, E.A., Riccio, G., Bone, F., Oliviero, U., Sacca, L., 2000. Cardiovascular effects of short-term growth hormone hypersecretion. J. Clin. Endocrinol. Metab. 85, 179–182.

Fazio, S., Sabatini, D., Capaldo, B., Vigorito, C., Giordano, A., Guida, R., Pardo, F., Biondi, B., Sacca, L., 1996. A preliminary study of growth hormone in the treatment of dilated cardiomyopathy. N. Engl. J. Med. 334, 809–814.

Frustaci, A., Chimenti, C., Setoguchi, M., Guerra, S., Corsello, S., Crea, F., Leri, A., Kajstura, J., Anversa, P., Maseri, A., 1999. Cell death in acromegalic cardiomyopathy. Circulation 99, 1426–1434.

Grimm, D., Cameron, D., Griese, D.P., Riegger, G.A., Kromer, E.P., 1998. Differential effects of growth hormone on cardiomyocyte and extracellular matrix protein remodeling following experimental myocardial infarction. Cardiovasc. Res. 40, 297–306.

Hoodless, P.A., Wrana, J.L., 1998. Mechanism and function of signaling by the TGF-β superfamily. Curr. Top. Microbiol. Immunol. 228, 235–272.

Ignotz, R.A., Massague, J., 1986. Transforming growth factor-β stimulates the expression of fibronectin and collagen and their incorporation into the extracellular matrix. J. Biol. Chem. 261, 4337–4345.

Iwami, K., Ashizawa, N., Do, Y.S., Graf, K., Hsueh, W.A., 1996. Comparison of ANG II with other growth factors on Egr-1 and matrix gene expression in cardiac fibroblasts. Am. J. Physiol. 270, H2100–2107.

Kuwahara, F., Kai, H., Tokuda, K., Kai, M., Takeshita, A., Egashira, K., Imaizumi, T., 2002. Transforming growth factor-β function blocking prevents myocardial fibrosis and diastolic dysfunction in pressure-overloaded rats. Circulation 106, 130–135.

Lieberman, S.A., Bukar, J., Chen, S.A., Celniker, A.C., Compton, P.G., Cook, J., Albu, J., Perlman, A.J., Hoffman, A.R., 1992. Effects of recombinant human insulin-like growth factor-I (rhIGF-I) on total and free IGF-I concentrations, IGF-binding proteins, and glycemic response in humans. J. Clin. Endocrinol. Metab. 75, 30–36.

Lopez-Velasco, R., Escobar-Morreale, H.F., Vega, B., Villa, E., Sancho, J.M., Moya-Mur, J.L., Garcia-Robles, R., 1997. Cardiac involvement in acromegaly: specific myocardiopathy or consequence of systemic hypertension? J. Clin. Endocrinol. Metab. 82, 1047–1053.

Lu, C., Schwartzbauer, G., Sperling, M.A., Devaskar, S.U., Thamotharan, S., Robbins, P.D., McTiernan, C.F., Liu, J.L., Jiang, J., Frank, S.J., Menon, R.K., 2001. Demonstration of direct effects of growth hormone on neonatal cardiomyocytes. J. Biol. Chem. 276, 22892–22900.

Mehrhof, F.B., Muller, F.U., Bergmann, M.W., Li, P., Wang, Y., Schmitz, W., Dietz, R., von Harsdorf, R., 2001. In cardiomyocyte hypoxia, insulin-like growth factor-I-induced antiapoptotic signaling requires phosphatidylinositol-3-OH-kinase-dependent and mitogen-activated protein kinase-dependent activation of the transcription factor cAMP response element-binding protein. Circulation 104, 2088–2094.

Morvan, D., Komajda, M., Grimaldi, A., Turpin, G., Grosgogeat, Y., 1991. Cardiac hypertrophy and function in asymptomatic acromegaly. Eur. Heart J. 12, 666–672.

Nakamura, H., Ueno, H., Yamashita, K., Shimada, T., Yamamoto, E., Noguchi, M., Fujimoto, N., Sato, H., Seiki, M., Okada, Y., 1999. Enhanced production and activation of progelatinase A mediated by membrane-type 1 matrix metalloproteinase in human papillary thyroid carcinomas. Cancer Res. 59, 467–473.

Osterziel, K.J., Strohm, O., Schuler, J., Friedrich, M., Hanlein, D., Willenbrock, R., Anker, S.D., Poole-Wilson, P.A., Ranke, M.B., Dietz, R., 1998. Randomised, double-blind, placebo-controlled trial of human recombinant growth hormone in patients with chronic heart failure due to dilated cardiomyopathy. Lancet 351, 1233–1237.

Penney, D.G., Dunbar Jr., J.C., Baylerian, M.S., 1985. Cardiomegaly and haemodynamics in rats with a transplantable growth hormone-secreting tumour. Cardiovasc. Res. 19, 270–277.

Rodrigues, E.A., Caruana, M.P., Lahiri, A., Nabarro, J.D., Jacobs, H.S., Raftery, E.B., 1989. Subclinical cardiac dysfunction in acromegaly: evidence for a specific disease of heart muscle. Br. Heart J. 62, 185–194.

Sacca, L., Cittadini, A., Fazio, S., 1994. Growth hormone and the heart. Endocr. Rev. 15, 555–573.

Schultz, J.E.J., Witt, S.A., Glascock, B.J., Nieman, M.L., Reiser, P.J., Nix, S.L., Kimball, T.R., Doetschman, T., 2002. TGF-β1 mediates the hypertrophic cardiomyocyte growth induced by angiotensin II. J. Clin. Invest. 109, 787–796.

Sigel, A.V., Centrella, M., Eghbali-Webb, M., 1996. Regulation of proliferative response of cardiac fibroblasts by transforming growth factor-β1. J. Mol. Cell. Cardio. 28, 1921–1929.

Takahashi, N., Calderone, A., Izzo Jr., N.J., Maki, T.M., Marsh, J.D., Colucci, W.S., 1994. Hypertrophic stimuli induce transforming growth factor-β1 expression in rat ventricular myocytes. J. Clin. Invest. 94, 1470–1476.

Tomita, H., Egashira, K., Ohara, Y., Takemoto, M., Koyanagi, M., Katoh, M., Yamamoto, H., Tamaki, K., Shimokawa, H., Takeshita, A., 1998. Early induction of transforming growth factor-β via angiotensin II type 1 receptors contributes to cardiac fibrosis induced by long-term blockade of nitric oxide synthesis in rats. Hypertension 32, 273–279.

Wrana, J.L., Attisano, L., Carcamo, J., Zentella, A., Doody, J., Laiho, M., Wang, X.F., Massague, J., 1992. TGF-β signals through a heteromeric protein kinase receptor complex. Cell 71, 1003–1014.

Yang, R., Bunting, S., Gillett, N., Clark, R., Jin, H., 1995. Growth hormone improves cardiac performance in experimental heart failure. Circulation 92, 262–267.

THE JOURNAL OF BIOLOGICAL CHEMISTRY
Vol. 278, No. 1, Issue of January 3, pp. 64–70, 2003
Printed in U.S.A.

Structural Divergence of Human Ghrelin

IDENTIFICATION OF MULTIPLE GHRELIN-DERIVED MOLECULES PRODUCED BY POST-TRANSLATIONAL PROCESSING*

Received for publication, May 30, 2002, and in revised form, September 26, 2002
Published, JBC Papers in Press, October 31, 2002, DOI 10.1074/jbc.M205366200

Hiroshi Hosoda‡§, Masayasu Kojima¶, Tsunekazu Mizushima‖, Shigeomi Shimizu, and Kenji Kangawa‡§‡‡**

*From the ‡Department of Biochemistry, National Cardiovascular Center Research Institute, Suita, Osaka 565-8565, the ¶Institute of Life Science, Kurume University, Kurume, Fukuoka 839-0861, the Departments of ‖Surgery and **Post-Genomics and Diseases, Osaka University Graduate School of Medicine, Suita, Osaka 565-0871, and the §Translational Research Center, Kyoto University Hospital, Kyoto, 606-8507, Japan*

Ghrelin, a novel 28-amino acid peptide with an *n*-octanoyl modification at Ser^3, was isolated from rat stomach and found to be an endogenous ligand for the growth-hormone secretagogue receptor (GHS-R). This octanoyl modification is essential for ghrelin-induced GH release. We report here the purification and identification of human ghrelin from the stomach, as well as structural analysis of the human ghrelin gene and quantitation of changes in plasma ghrelin concentration before and after gastrectomy. Human ghrelin was purified from the stomach by gel filtration and high performance liquid chromatography, using a ghrelin-specific radioimmunoassay and an intracellular calcium influx assay on a stable cell line expressing GHS-R to test the fractions. In the course of purification, we isolated human ghrelin of the expected size, as well as several other ghrelin-derived molecules. Classified into four groups by the type of acylation observed at Ser^3; these peptides were found to be non-acylated, octanoylated (C8:0), decanoylated (C10:0), and possibly decenoylated (C10:1). All peptides found were either 27 or 28 amino acids in length, the former lacking the C-terminal Arg^{28}, and are derived from the same ghrelin precursor through two alternative pathways. The major active form of human ghrelin is a 28-amino acid peptide octanoylated at Ser^3, as was found for rat ghrelin. Synthetic octanoylated and decanoylated ghrelins produce intracellular calcium increases in GHS-R-expressing cells and stimulate GH release in rats to a similar degree. Both ghrelin and the ghrelin-derived molecules were found to be present in plasma as well as stomach tissue. Plasma levels of immunoreactive ghrelin after total gastrectomy in three patients were reduced to approximately half of their pre-gastrectomy values, after which they gradually increased. This suggests that the stomach is the major source of circulating ghrelin and that other tissues compensate for the loss of ghrelin production after gastrectomy.

Growth hormone (GH)[1] secretion from the pituitary gland is regulated by two hypothalamic hormones, growth hormone-releasing hormone and somatostatin (1, 2). A third independent pathway responsible for regulation of GH release has recently emerged from studies of artificial GH secretagogues (GHSs) (3, 4). GHSs are synthetic compounds that are potent stimulators of pituitary GH release, acting through the GHS receptor (GHS-R) (5–7). Previously, we identified ghrelin, an endogenous ligand for GHS-R, from rat stomach (8). Ghrelin, a 28-amino acid peptide capable of stimulating GH release *in vitro* and *in vivo*, has a unique *n*-octanoyl modification at its third serine residue (Ser^3), which is essential for this function (9–11). Subsequently, des-Gln^{14}-ghrelin, also isolated from rat stomach, was identified as a second endogenous ligand for GHS-R (12). Des-Gln^{14}-ghrelin is produced from the ghrelin gene by an alternative splicing mechanism and is also octanoylated at Ser^3.

In the present study, we purified human ghrelin from the stomach, using a ghrelin-specific radioimmunoassay (RIA) (13) and an intracellular calcium influx assay on a stable cell line expressing GHS-R (8, 12). During the course of purification, we noticed several minor peptides with characteristics different from standard ghrelin that displayed ghrelin-like activity. We identified these stomach peptides as ghrelin-derived molecules and examined the levels of ghrelin as well as these ghrelin-derived molecules in human plasma.

The ghrelin gene is abundantly expressed in rat (8) and human (14) stomach, and in the rat, no other major sources of ghrelin production have been observed (13, 15). These results prompted us to question whether ghrelin should be drastically reduced following gastrectomy. To address this question, we examined the change in plasma levels of immunoreactive ghrelin (ir-ghrelin) in humans before and after total gastrectomy.

EXPERIMENTAL PROCEDURES

Radioimmunoassays for Ghrelin—RIAs specific for ghrelin were performed as previously described (13). In rabbits two types of polyclonal antibodies were raised against the N-terminal fragment (Gly^1-Lys^{11} with *O-n*-octanoylation at Ser^3) and the C-terminal fragment (Gln^{13}-Arg^{28}) of rat ghrelin. The RIA incubation mixture consisted of 100 μl of standard ghrelin or unknown sample, and 200 μl of antiserum diluted with RIA buffer (50 mM sodium phosphate buffer (pH 7.4), 0.5% bovine

* This work was supported by grants from the Ministry of Education, Science, Sports and Culture of Japan, the Ministry of Health, Labor and Welfare of Japan, the Promotion of Fundamental Studies in Health Science from the Organization for Pharmaceutical Safety and Research of Japan, and the Takeda Science Foundation. The costs of publication of this article were defrayed in part by the payment of page charges. This article must therefore be hereby marked "*advertisement*" in accordance with 18 U.S.C. Section 1734 solely to indicate this fact.

The nucleotide sequence(s) reported in this paper has been submitted to the GenBank™/EBI Data Bank with accession number(s) AB029434 and AB035700.

‡‡ To whom correspondence should be addressed: Dept. of Biochemistry, National Cardiovascular Center Research Institute, 5-7-1 Fujishirodai, Suita, Osaka 565-8565, Japan. Tel.: 81-6-6833-5012; Fax: 81-6-6835-5402; E-mail: kangawa@ri.ncvc.go.jp.

[1] The abbreviations used are: GH, growth hormone; GHS, growth hormone secretagogue; GHS-R, growth hormone secretagogue receptor; RIA, radioimmunoassay; ir, immunoreactive; CHO, Chinese hamster ovary; $[Ca^{2+}]_i$, intracellular calcium concentration; AcOH, acetic acid; CM, carboxymethyl; RP, reverse-phase; HPLC, high-performance liquid chromatography; ESI-MS, electrospray ionization mass spectrometry; N-RIA, N-terminal fragment of rat ghrelin-(1–11); C-RIA, C-terminal fragment of rat gherlin-(13–28).